WATER PURIFICATION USING PHOTOCATALYSIS, OZONATION AND ULTRAVIOLET DISINFECTION

TSOI CHI CHUNG

MPhil

The Hong Kong Polytechnic University

2018

THE HONG KONG POLYTECHNIC UNIVERSITY

DEPARTMENT OF APPLIED PHYSICS

WATER PURIFICATION USING PHOTOCATALYSIS, OZONATION AND ULTRAVIOLET DISINFECTION

TSOI Chi Chung

A thesis submitted in partial fulfilment of the

requirements for the degree of Master of Philosophy

AUGUST, 2017

CERTIFICATE OF ORIGINALITY

I hereby declare that this thesis is my own work and that, to the best of my knowledge and belief, it reproduces no material previously published or written, nor material that has been accepted for the award of any other degree or diploma, except where due acknowledgement has been made in the text.

_____ (Signature)

TSOI Chi Chung (Name of candidate)

ABSTRACT

The rapid urbanization is creating a rising demand of clean water while producing a huge amount of wastewater. A special issue in Hong Kong is that sea water is extensively used for toilet flushing and street cleaning, which generate contaminated sea water. Wastewater treatment plants often rely on physical, chemical and biological methods to remove the contaminants, but the state of the art is still limited by several technical challenges. For instance, (1) many dissolved toxic chemicals (e.g., detergents) cannot be treated efficiently by the prevailing treatment methods; (2) the treated wastewater still contains significant amounts of residual chemicals and bacteria, which will affect water activities; (3) the contaminated sea water cannot be cleaned effectively using those methods developed for the contaminated freshwater. The high concentration of salt ions affects the microorganism growth and the flocculation in the treatment pools.

This study aims to overcome the existing challenges using solar photocatalysis, ultraviolet (UV) irradiation, ozone and their combined effects. More specially, this research consists of three parts: (1) solar photocatalytic reactors to degrade organic pollutants in freshwater, (2) photocatalytic ozonation of sea water and (3) UV ozonation of residual bacteria in wastewater effluent. The logic behind is that sunlight is abundant while photocatalysis can decompose a wide range of chemicals, and thus the solar photocatalysis is energy-saving and environmental friendly. In sea water, the existence of Na^+, Cl^- and other ions invalidates many biochemical methods and reduces the efficiency of photocatalysis; nevertheless, the addition of ozone produces OH^* radicals, enhances the capture of photoexcited electrons, and at the same time, provides dissolved O_2 to improves the photodegradation. To kill bacteria, UV irradiation and ozonation each has its own weaknesses, but the successive use of both can well complement each other to

kill the bacteria more effectively.

The first part of this research starts with a chip-size solar reactor (footprint of reaction chamber 1 cm × 1 cm) for the laboratory tests and mechanism studies. Then, it is scaled up to the meter size (footprint of reaction chamber 60 cm × 40 cm). It is made of PMMA plates. A simple soaking and spraying method has been developed to form the TiO_2 film on the PMMA, which is the first method that can make large-area, uniform photocatalytic film on cheap, durable, lightweight and non-brittle substrates. Field tests show that the large-size reactor can degrade MB by 30% in sunlight for two hours, which is 23.6 times faster than the photolysis. Although the performance has much room to improve, this large solar reactor is the first demonstration of the planar reactor directly scaled up from the microfluidic reactor; and it also moves one step forward to process large amount of water sample that is a typical requirement of practical applications.

The second part of this research synergizes photocatalysis and ozonation for the decontamination of sea water. Mechanism studies and experiments using a home-made setup show that the maximum synergistic effect is achieved when the ozone concentration is about 50 ppm. Under this condition, the reaction rate is improved by more than 2 times as compared to that of only photocatalysis. This is the first study of sea water decontamination using the photocatalytic ozonation and is worth further development to tackle the existing waste sea water problem in Hong Kong.

The third part aims to solve another problem of the treated waste water, the residual bacteria in the effluent, which result from the extensive uses of various types of bacteria in the biological treatment method. The effluent often has E. coli > 100 cfu/mL. To reduce the count to < 10 cfu/mL with minimal cost, the UV irradiation is first applied to damage the nucleic acids inside the bacteria, followed by the ozonation to destroy the external membrane of bacteria. The combined effect enables to completely kill the bacteria and

prevents the resurrection of bacteria under visible irradiation, which is a common problem of UV-only treatment. This work has developed a new gas-liquid exchange plant for fast dissolution of ozone in the water sample. Experiments start with the sample of 3×10^6 cfu/mL and obtain 46 cfu/mL right after the UV irradiation for 0.6 s, 270 cfu/mL if the UV-irradiated sample is then irradiated by visible light for 24 hours, and < 5 cfu/mL if the UV-irradiation is followed by the 5-ppm ozonation and the 24-h visible irradiation. The large difference between 270 cfu/mL and < 5 cfu/mL shows that a low concentration of ozone is already able to reduce the bacteria count by a factor of more than 50. As the UV irradiation time is short and the ozone concentration is low, the electricity cost is estimated to be HK$0.15 for the treatment of 1 ton of water.

In summary, this M. Phil. study has three major contributions to science and applications: the new solar reactors for the photocatalytic degradation of residual chemicals in waste fresh water, the photocatalytic ozonation method for the decontamination of waste sea water and the UV ozonation for killing the residual bacteria in the wastewater effluent. The novelty and originality of this work lie most in the new design of solar reactors, the first study of photocatalytic ozonation of sea water and the new design of gap-liquid exchange plant for the disinfection of residual bacteria. The designs and techniques developed in this work are of highly application values and may be incorporated into the current wastewater treatment works.

ACKNOWLEDGMENTS

I would like to express my sincerest appreciation to my chief supervisor **Dr. Xuming ZHANG** and co-supervisor **Dr. Polly, Hang Mei LEUNG** in Department of Health Technology and Informatics in The Hong Kong Polytechnic University. Without their excellent guidance, constant encouragement and support during the past two years of my M. Phil. study, it would be impossible for me to complete my research work. Their high standard, profound academic insight and inspired discussions contribute greatly to improve the quality of my doctorial research.

I would also like to thank Dr. Yuen Hong TANG, Mr. Kai Hong HO, Ms. Yiu YUENG, Mr. Tsz Lam CHAN and Ms. Wing Man HO in Department of Applied Physics in The Hong Kong Polytechnic University for their assistance on my postgraduate research.

Besides, I would like to thank all the past and present group members for their great help and friendship, including Mr. Qingming CHEN, Dr. Xiaowen HUANG, Dr. Furui TAN, Dr. Tenghao LI, Miss Yujiao ZHU, Mr, Pui Hong YUENG and Dr. Ning WANG.

Finally, I would like to thank my family and my girlfriend, Miss Wing Yan CHENG for their support on my study and life.

TABLE OF CONTENTS

LIST OF FIGURES

LIST OF TABLES

LIST OF PUBLICATIONS

Journal Publications

1. Ning Wang, Furui Tan, **Chi Chung Tsoi** and Xuming Zhang*, Photoelectrocatalytic microreactor for seawater decontamination with negligible chlorine generation, Microsystem Technologies, vol. 1, 21 Nov 2016. *DOI: https://doi.org/10.1007/s00542-016-3193-8.*
2. Furui Tan, Tenghao Li, Ning Wang, Sin Ki Lai, **Chi Chung Tsoi**, Weixing Yu, Xuming Zhang*, Rough gold films as broadband absorbers for plasmonic enhancement of TiO2 photocurrent over 400 – 800 nm, Scientific Reports, vol. 6, paper no. 33049, 9 Sep 2016. *DOI: 10.1038/srep33049.*
3. Ning Wang, Furui Tan, Yu Zhao, **Chi Chung Tsoi**, Xudong Fan, Weixing Yu & Xuming Zhang*, Optofluidic UV-Vis spectrophotometer for online monitoring of photocatalytic reactions, Scientific Reports, vol. 6, paper no. 28928, 29 Jun 2016. *DOI:10.1038/srep28928.*

Conference papers

1. **Chi Chung Tsoi**, Pui Hong Yeung and Xuming Zhang*, Solar reactor for photocatalytic water purification, The 7th International Multidisciplinary Conference on Optofluidics (**IMCO2017**), 25 – 28 July 2017, Singapore, paper sciforum-012821. (**Best Poster Award)**
2. Pui Hong Yeung, **Chi Chung Tsoi**, Ning Wang and Xuming Zhang*, Photocatalytic water purification by using nanomaterial and solar reactor, The 7th International Multidisciplinary Conference on Optofluidics (**IMCO2017**), 25 – 28 July 2017, Singapore, paper sciforum-011422.

3. **Chi Chung Tsoi**, Pui Hong Yeung, Ning Wang and Zhang Xuming, Decontamination of Sea Water using Photocatalytic Ozonation, The 5th European Conference on Environmental Applications of Advanced Oxidation Processes (**EAAOP2017**), 25-29 June 2017, Czech Republic.
4. Pui Hong YEUNG, **Chi Chung TSOI**, Ning WANG and Xuming ZHANG *, Photocatalytic water purification by plasmonic nanomaterials and solar reactor, The 5th European Conference on Environmental Applications of Advanced Oxidation Processes (**EAAOP2017**), 25-29 June 2017, Czech Republic.
5. **Chi Chung Tsoi** and Xuming Zhang*, Photocatalytic Ozonation for Sea Water Treatment, The 19th Annual Conference of the Physical Society of Hong Kong (**PSHK2016**), 3–4 June 2016, Hong Kong.
6. Ning Wang, Furui Tan, **Chi Chung Tsoi** and Xuming Zhang, Microfluidic reactors for photocatalytic conversion of solar energy into chemical energy, The 8th International Symposium on Microchemistry and Microsystems (**ISMM2016**), 30 May – 1 June 2016, Hong Kong.
7. Ning Wang, Furui Tan, **Chi Chung Tsoi** and Xuming Zhang, Integrated optofluidic device with on-chip UV-Vis spectrophotometer for online monitoring of photocatalytic reactions, The 8th International Symposium on Microchemistry and Microsystems (**ISMM2016**), 30 May –1 June 2016, Hong Kong.
8. N. Wang, F. R. Tan, **C. C. Tsoi** and X. M. Zhang, Optofluidic microreactors for visible-light photocatalysis, The Conference on Lasers and Electro-Optics (**CLEO2015**): Laser Science & Applications, 10 – 15 May 2015, San Jose, CA, USA, paper AW4K.3.
9. X. W. Huang, Y. J. Zhu, **C. C. Tsoi**, X. M. Zhang, Experimental study on microfluidic nanoparticle immobilization using a biomimetic method, Symposium

on Design, Test, Integration and Packaging of MEMS/MOEMS (**DTIP 2015**), 27 - 30 April 2015, Montpellier, France.

LIST OF AWARDS

1. **Best paper award**, 7th International Multidisciplinary Conference on Optofluidics 2017, Singapore, 2017.
2. **Reaching Out Award**, The Hong Kong Special Administrative Region Government Scholarship Fund, 2016.
3. **Talent Development Scholarship**, The Hong Kong Special Administrative Region Government Scholarship Fund, 2016.
4. **National Second prize (國家二等獎)**, The 14th "Challenge Cup" national university students extracurricular academic and technical competition ("挑戰杯"全國大學生課外學術科技作品競賽), Central Committee of the Communist Youth League, Science and Technology Association of China, Ministry of Education and the National Student Union (共青團中央,中國科協,教育部和全國學聯), 2015.

CHAPTER 1. INTRODUCTION

1.1 Background

From 1760s, industry revolution began to develop, making the mass production a standard. Since then, the pollution problem became more and more serious. The fundamental problem is the water pollution, mainly resulting from three industrial sections: textiles, steam power and iron making.

In textiles, the power loom increases the output of a worker by a factor of over 40% and demands more water for bleaching and dyeing. The waste water from bleaching and dyeing contains dye and phosphorus compounds. Those materials are kinds of nutrient for bacteria to breed and thus pollute the environment further. On the other hands, the demand of coal has been increased since the innovation of steam power. The cinder may mix with the steam and disperse into river. However, the cinder-containing water is a good medium for bacteria breeding, which would reduce the concentration of oxygen in water and threaten the aquatic creatures. The last innovation is iron making. The demand of water for cooling has been increasing since the start. In the iron making, some toxic chemicals are used and released into the cooling water and then the water circulation, which would kill the top-level animals.

Rome and England were among the first regions that developed waste water treatment system in 1762. They added limestone and metal salts into the waste water to neutralize and precipitate some kinds of chemicals, which would be removed from the waste water. And that technology is called the first level treatment technology nowadays.

In the middle of 18th century, there was the second industrial revolution. And the main pollutant of the waste water changed from chemical pollutants to organic pollutants. In 1881, the first biological treatment reactor was developed. And active sludge was also developed in 1914. This treatment technology is still being used nowadays.

From the first industrial revolution till now, the main industry has been changed and the main pollutants have also been changed. After 2000, the abuse of antibiotics, pesticide, and the illegal emission of amine and disinfectants cause the biological treatment method to be ineffective. In addition, the concentration of pollutants in waste water is increasing and new pollutants appear, it is the time to review the available water treatment methods and to develop new methods.

The first level treatment often adds chemicals to neutralize waste water and to precipitate some elements. However, the first level treatment may create secondary pollution due to the addition of chemicals and cannot handle the organic pollutants efficiently. This called for the second level treatment method, which is still being in used the water treatment works in Hong Kong, Mainland, China, United States and other developed countries. The second level treatment method uses bacteria to digest the organic pollutants. However, the bacteria need to be disinfected in the final stage, before the effluent is dispersed into the surface water. If the sterilization is not enough, high concentration of bacteria water would enter river and threaten the water safety. The rapid development of living standard requires higher water quality and lower bacteria concentration in the river, these call for the development of the third level treatment method. This method is a kind of physical method, photocatalysis. In the photocatalysis process, many free radicals are produced when photons with sufficient energy are

absorbed by the semiconductor photocatalyst. The highly oxidative free radicals would oxidize most of the organics and even the inorganic materials. Photocatalysis would be a solution in the future to solve the water pollution problem. However, photocatalysis itself is not efficient for sea water since the salt ions in sea water adversely affect the redox reaction in photocatalysis. New method should be developed, like the photocatalytic ozonation to be presented in this M. Phil. study.

1.2 Objectives

The major objective of my study is to develop new water treatment methods to solve the prevailing problems of the state of the art, including solar reactors, photocatalytic ozonation for seawater decontamination and UV-ozone disinfection.

1.3 Organization of thesis

Chapter 1 presents the general background of this research study.

Chapter 2 will give a detailed review of the relative materials and methods to be used in this research.

Chapter 3 will present the first work of this M. Phil. Study – a new design of planner solar reactor. A small chip-size reactor will be fabrication for laboratory tests and mechanism study, and a large-size solar reactor for field test.

Chapter 4 will present the second work of this research – a new photocatalytic ozonation method for the decontamination of waste sea water. Synergistic effect of photocatalysis and ozonation is also one of the focus of this study.

Chapter 5 will present the third work of this research – a UV-ozone combined method for the complete disinfection of waste water effluent from the treatment works.

Chapter 6 will conclude the research achievements of this M. Phil. study and will suggest some worthful topics for future studies.

CHAPTER 2. LITERATURE REVIEW

This chapter will present a general review of the materials and methods that serve the technical bases for our research studies to be presented in next three chapters. The first part of my literature review is to study the principle of photocatalysis since it will be involved in two chapters of my study. Different kinds of photocatalysts will be discussed to find the suitable materials for my study. Furthermore, various design of photocatalytic reactors will be reviewed. Next, previous studies will be reviewed on the influence of salt ions on photocatalysis and the reaction between ozone and NaCl solution. At the end, the disinfection techniques for waste water will be reviewed.

2.1 Principle of photocatalysis

2.1.1 Photoexcitation of electron-hole pair

As shown in the left part of **FIGURE 2.1**, When the photon energy is greater than the band gap of semiconductor photocatalyst, photon would be absorbed to excite electrons in the valance band to the conduction band, forming a conduction band electron (e^-), and leaving a hole in the valence band (h^+).[1] Due to the discontinuity of the semiconductor energy band, photo-exited electrons and holes have long life time, they can diffuse to the surface of the photocatalyst particles and react with the adsorbed molecules / ions on the

surface for redox reactions.[2]

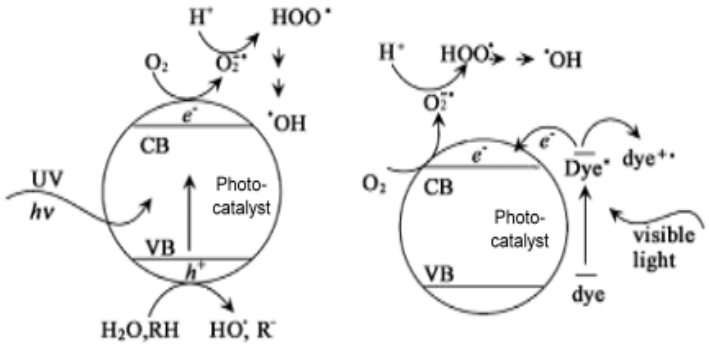

FIGURE 2.1 Mechanism of photocatalysis using semiconductor photocatalyst.

2.1.2 Oxidation and reduction reactions

Some photo-excited holes and electrons in the interior or the surface of the photocatalytic particles may also experience direct recombination. The remaining holes on the surface of photocatalytic particle can be captured by the adsorbed OH^- or H_2O to generate HO^* radicals, which is highly active for non-selective oxidation of a variety of organic compounds and mineralization. On the other hands, photon-excited electrons can be captured by the adsorbed O_2 molecule to generate HO_2 and O_2^{*-}, these reactive oxygen free radicals can participate redox reactions. The process is shown in **FIGURE 2.1**, using the following reaction formula [3]–[5]:

$$\text{Photocatalyst} + h\nu \rightarrow \text{Photocatalyst}(e^-, h^+) \quad (2.1)$$

$$e^- + h^+ \rightarrow \text{heat or } h\nu \quad (2.2)$$

$$h^+ + \text{OH}^-_{\text{ads}} \rightarrow \text{HO}^* \quad (2.3)$$

$$h^+ + \text{H}_2\text{O}_{\text{ads}} \rightarrow \text{HO}^* + \text{H}^+ \quad (2.4)$$

$$e^- + \text{O}_2 \rightarrow \text{O}_2^{*-} \quad (2.5)$$

HO^* can oxidize electron donor (D), and electronic receptors can restore it. In addition, h^+ can also directly oxidize organic matter:

$$\text{HO}^* + \text{D} \rightarrow \text{D}^{*+} + \text{H}_2\text{O} \quad (2.6)$$

$$e^- + \text{A} \rightarrow \text{A}^{*-} \quad (2.7)$$

$$h^+ + \text{D} \rightarrow \text{D}^{*+} \quad (2.8)$$

Low quantum efficiency of photocatalytic reaction (~ 10^{-2}) [1] is one of the most critical problems for practical applications. Quantum efficiency of photocatalytic reaction depends on the carrier recombination rate, which in turn mainly depends on two factors: the carrier trapping process inside the photocatalyst; and the carrier migration process to the surface. Decreasing the carrier trapping or enhancing the surface charge transport can suppress the charge carrier recombination and thus increase the quantum efficiency of the photocatalytic reactions. Typically, the electron and hole recombination is quick, at a rate of about 10^{-9} s, and the carriers are trapped at relatively slow rate, typically in 10^{-7}-10^{-8}

s.[6] Therefore, in order to effectively capture electrons or holes, it is important to pre-adsorb the capturing agent on the photocatalytic surface.

2.2 Study of photocatalytic materials

Titanium dioxide is a common photocatalytic material in the past 40 years. Currently, quantum chemistry calculation is the main method to evaluate the novel photocatalytic materials. This is because theoretical calculations can clearly understand the electronic structure of semiconductor photocatalytic materials, band information and photocatalytic reactions factors. Under the calculation, a number of new photocatalytic materials have been designed and studied.

In recent decades, the photocatalytic materials have been greatly enriched, and can be roughly classified into the following categories: titanium dioxide, bismuth containing composites material, cadmium sulfide, and other.[7]

2.2.1 Titanium dioxide (TiO_2)

Photocatalytic oxidation using TiO_2 began in 1972 when Fujishima and Hondo reported TiO_2 absorb light radiation in a solar cell to generate hydrogen gas by reduction reaction of aqueous [8]. In late 1970s, a number of literatures reported the usage of photocatalysis treatment of various pollutants in the waste water, involving a variety of important chemicals, such as: phenolic compounds, hydrocarbons, surfactants, organic paints and

some inorganic compounds.

The n-type TiO_2 semiconductor is highly chemical stable, photo-corrosion resistive, insoluble, and having a deep valence band energy level. In addition, TiO_2 is abundant non-toxic and low cost. Therefore, it is widely used as a photocatalyst for photocatalytic oxidation reactions. [9]–[11]

2.2.2 Bismuth containing composite materials

A series of complex oxides containing bismuth have shown good catalytic properties under visible light. They form a new type of photocatalytic materials, which has recently become a hot topic in the field of photocatalysis. The three of most famous composites are bismuth tungstate, bismuth vanadium oxide, bismuth molybdate [12], [13].

(1) Bismuth Tungstate (Bi_2WO_6)

Bi_2WO_6 has a strong optical absorption in the visible region since its band gap is smaller than TiO_2. According to theoretical calculations, band gap of Bi_2WO_6 is about 1.63 eV. However, many reports show Bi_2WO_6 with 1.63 eV cannot be made easily. Kudo et al. [14] found that Bi_2WO_6 doping $AgNO_3$ can absorb visible light and split water to produce O_2. Zou et al. [15] reported Bi_2WO_6 can effectively degrade $CHCl_3$ and CH_3CHO under visible light with the wavelengths > 440 nm. Zhu, et al. [16] prepared a large area nano Bi_2WO_6 film using Na_2WO_4 and $Bi(NO_3)_3$ as raw materials, the prepared Bi_2WO_6 has a

band gap of 2.75eV . [12], [17]

(2) Bismuth Vanadium Oxide ($BiVO_4$)

There are three different crystal phases of $BiVO_4$: tetragonal zircon phase (zt phase), tetragonal scheelite phase (st phase) and monoclinic scheelite phase (m phase). Energy band gap of $BiVO_{4(zt)}$ is about 2.9 eV[18], which can adsorb only ultraviolet light. The energy band gap of $BiVO_{4(st)}$ and m-$BiVO_4$ are 2.34 eV and 2.41 eV, respectively [19]. The latter two $BiVO_4$ crystalline phases are responsive to visible light, with the band-edge at about 550nm, the center portion of visible light. Therefore, $BiVO_4$ is highly efficient for sunlight. The photocatalytic performance under visible light conditions is mainly determined by their valence band structure differences, $BiVO_{4(zt)}$, $BiVO_{4(st)}$ and m-$BiVO_4$.

Kudo et al. [20] reported that m-$BiVO_4$ has a high water photolysis of oxygen evolution activity under visible light irradiation, when silver nitrate sacrificial agent. When the presence of water, the electron acceptor, such as Ag^+, or Fe^{3+}, the photon generating conduction band electrons are consumed them to promote the release of O_2 reaction.[13]

(3) Bismuth Molybdate (Bi_2MoO_6)

The structures of Bi_2MoO_6 and Bi_2WO_6 are similar. Their energy band gap is 2.33–2.59

eV. Kudo et al. [21] reported the photocatalytic properties of Bi_2MoO_6 in decomposition of water under visible light, and conducted systematic studies on the influence of energy band structure and crystalline on the photocatalytic performance. [12], [17]

2.2.3 Cadmium sulfide (CdS)

Cadmium sulfide also is one of the popular materials for water purification. Zhai [20] showed that the performance of degradation of acid fuchsine for the peak at 543 nm which increased very quickly once the branched CdS nanowires were added. The experiment results suggested that the branched CdS nanowires might have a high BET surface and thus could absorb the dye molecules more efficiently. Under increasing exposure time, the typical sharp peak at 543 nm diminished gradually and completely vanished after 45 min. [20], [22], [23]

2.2.4 Others

The other new photocatalytic materials development methods focused on the two directions. One is to develop the material of narrow band gap for better visible response. The other is to develop visible-responsive material by doping or heterostructure. These materials include cuprous oxide(Cu_2O), graphene-doped CdS, doped TiO_2, and plasmonic photocatalysts (e.g. Au/TiO_3, Ag/TiO_2). [10], [11], [24]–[28]

TABLE 2. 1 summarizes and compares the common photocatalytic materials in

different aspects such as the band gaps, the cut-off wavelength, the advantages and disadvantages.

TABLE 2. 1 Comparison of different photocatalysts.

Groups	Material	Band gap (eV)	Cut-off wavelength (nm)	Advantages	Disadvantages
Titanium	TiO_2	2.98-3.26	416	Highly stable, non-toxic, low cost	Optical absorption only in the UV region
Bismuth	Bi_2WO_6	1.63-2.75	760	Responsive to both visible and UV light	Photocorrosion, not stable
	$BiVO_4$	2.34-2.9	529		
	Bi_2MoO_6	2.33-2.59	532		
Cadmium	*CdS*	2.07-2.38	496	Responsive to both visible and UV light	Photocorrosion, not stable, potentially heavy metal toxic

2.3 Review of photocatalytic reactors

The two main aspects of photocatalytic reactor are the reactor design and the film fabrication. Proper deigns can effectively improve the reactor performance and reduce the cost for potential industry mass production.

2.3.1 Design of reactors

Photocatalytic reactor design is the core part of the photocatalytic treatment of pollutants.

Earliest photocatalytic reactor was designed for laboratory research, it has simple structure and is easy to operate. The reactor body is an open container, and allows to easily adjust the reaction liquid under the fluorescent lamp or UV light irradiation, and the distance between the lamp and the liquid surface. Nowadays, the design of reactor aims primarily at industry mass production for daily usage. Three most popular designs are fluidized photocatalytic reactor (FPR), water film photocatalytic reactor (WFPR) and fixed film photocatalytic reactor (FFPR).

(1) Fluidized photocatalytic reactor (FPR)

The FPR often uses TiO_2 particles in a suspension for high photocatalytic degradation efficiency. But it is difficult to recycle the photocatalytic powders.

Ochuma developed the pilot contact down-flow reactor, the upper part is a solid-liquid-gas mixing zone, the lower is the photocatalysis reaction zone, using an internal vertical mounting of 1.0 kW ultraviolet lamp. The reactor has a very high mass transfer efficiency. Under optimum conditions, the initial concentration of 100 mg/L 1,8-Diazabicyclo [5.4.0] undec-7-ene ($C_9H_{16}N_2$) solution can be completely degraded within 45 min. [29]–[35]

(2) Water film photocatalytic reactor (WFPR)

The WFPR can form a liquid film in the photocatalytic reactor to improve the mass

transfer and the light absorption and to enhance the photocatalytic degradation efficiency.

Dionysius et al. developed a semicircular reactor TiO_2 by fixing onto the surface of the turntable, which is placed vertically in the middle of the reactor. A part is immersed in the reaction mixture, and the other part is exposed to the air. When the turntable is rotated, the reaction liquid is brought into a water film formed on the turntable; the water film thickness can be adjusted by the rotation speed. Experimental results showed that the photocatalytic degradation of pentachlorophenol (PCP) up to 90%, after the reaction of 350 h. [29], [31], [32], [36]–[44]

(3) Fixed film photocatalytic reactor (FFPR)

The FFPR fixs photocatalytic material to the container wall or other a suitable carrier, avoiding the recovery and reuse problem of photocatalyst, but it usually suffers from the problems of low amount of the photocatalyst and small surface area.

Krysova et al. designed a plate-type reactor using the PMMA sheet. The photocatalyst is a TiO_2 film coated on a glass plate, whose inclination angle can be adjusted. A UV light source is hanged 10 cm above the glass sheet. The liquid flows through the TiO_2 film on the square plate surface. Experiments showed the pollutant diuron concentration of decreased rapidly, and finally reduced completely degradation.

Damodar et al. used a similar film photocatalytic reactor, to treat four kinds of dyes

(reactive orange, active blue, black and acid reactive turquoise). Under sunlight for 5 ~ 6 h, the decolorization rate reached 90% to 98%.[29], [30], [35], [36], [39]–[42], [45]–[48]

2.3.2 Fabrication of photocatalytic thin film

Many types of photocatalytic carriers have been developed, each has certain its advantages and disadvantages. Loading method of photocatalytic materials need to consider the properties of the carrier type, the characteristics and the scope. [49]

(1) Impregnation sintering

Impregnation sintering process can be used to support photocatalytic material. The first step is to prepare the sol, and then the plate is immersed in the sol for a long time, and finally, it is calcined to form the photocatalytic materials. However, this method may cause uneven film distribution, an even crack in some places. It is necessary to repeat the coating. [9], [49]

(2) Spray pyrolysis

Spray pyrolysis method is simple, low cost, easy to operate, and suitable for large-scale continuous production. The first step is to dissolve the reactants. Then thin films is formed on the substrate surface by atomizing fine droplets with spraying on a hot substrate. The film quality is controlled by adjusting the spray volume, the spray distance

and the droplet size. [49], [50]

(3) Sol-gel method

The raw materials of sol-gel method are generally titanium alkoxide, and ethanol. Then many other components are added, such as water, organic acids and polymeric additives. They are mixed to get a stable sol. After coating and calcination, the photocatalytic film is deposited on various carriers. The TiO_2 film fabricated by this method is usually compact, dense and difficult to fall off. Calcination temperature and are important factors to control the crystal phase and the film thickness. [49]

(4) Direct attachment method

The direct attachment method connects the catalyst and the coupling agent directly since it uses the affinity between the nano-particles and the carrier. This method is simple, low cost, but the attachment is often weak, and easy to fall off. Therefore catalysts has short life time, making it not suitable for industrial applications. [49]–[51]

2.4 Influence of salt ions on photocatalysis

Photocatalytic decontamination relies on the photo-excited electrons and holes to initiate the redox reactions on the catalyst surface [52]–[53]. This is relative simple in fresh water. In sea water, things ae every different. For instance, the activities of photocatalyst would decrease significantly in sear water due to the salt ions and the suspended solids. [54]–[56].

Only a few studies have focused on the real application of the photocatalytic degradation of organic material in water. Such studies have indicated that the photocatalytic degradation in the presence of TiO_2 with UV irradiation can degrade antibiotics in water [57]–[59]. However, the salinity in water reduces the biodegradation and photodegradation of organic pollutant in water [60]. Seawater contains various inorganic ions such as Na+ and Cl^- ions, and also includes numerous other ions in minor concentrations (e.g., Ca^{2+}, Mg^{2+}, K^+, I^- , SO_4^{2-} and Br^-). To date, in-depth studies on effects of salinity and its constituents on the photocatalysis of antibiotics remain scarce.

The most abundant dissolved ions in seawater are sodium and chloride. Therefore, Yang chose and added NaCl to the solutions for a photocatalytic study of the same salinity levels as in the seawater to elucidate the ion effects of NaCl [61]. It is found that the photocatalytic degradation of the pollutant in the NaCl solution was significantly

faster than that in the seawater with the identical salinity. The results revealed that NaCl in seawater is not the only agent that weakens the photocatalytic degradation of the pollutant. Other dissolved ions in seawater (such as Mg^{2+}, Ca^{2+}, Br^{-}, SO_4^{2-}) might also contribute to the weakening effects in the photocatalytic degradation of the pollutant. In the following investigation, more cations and anions in seawater will be examined to study their effects on the photocatalytic degradation of the pollutants.

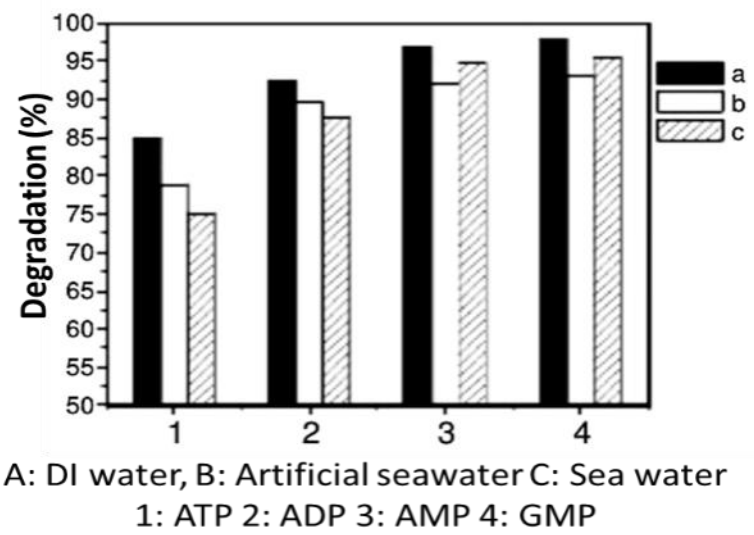

FIGURE 2.2 Comparative study of photocatalytic degradation of ATP, ADP, AMP and GMP in pure water, artificial sea water and real sea water [62].

On the other hands, Wang also studied and compared the photocatalytic efficiencies in pure water, sea water and artificial sea water. He chose adenosine monophosphate

(AMP), adenosine diphosphate (ADP), adenosine triphosphate (ATP) and GMP (aquatic organisms and organic phosphorus metabolism major product intermediates) as the degradation targets [62]. It can be seen from **FIGURE 2.2** that the photocatalytic efficiencies of the artificial sea water and the real sea water have been significantly reduced as compared to the DI water. This trend is valid for all target pollutants.

2.5 Ozonation in seawater

Dissolved ozone in NaCl solution is often used for water disinfection in sea aquariums and seawater swimming pools [63], as ozone saturated ice to store fish in the sea [64], and for treating patients with ozonated isotonic solutions [65]. Solutions of ozone in water are unstable, dissolved ozone is decomposed rather fast (half-life ~0.5–30 h, depending on the water purity [66]). In the NaCl solutions, the decomposition is even faster. Its rate depends considerably on the NaCl concentration [67]. Despite the apparent simplicity, there is still no clear understanding of ozone destruction in solutions of NaCl.

Oxygen is known to be the major reaction product and elemental chlorine is detected in the reaction mixture [68]. There is an assumption that hypochlorite (ClO^-) and chlorate (Cl-) would be formed [69]. Generally, the most accepted mechanism is reflected by reactions (2.9)–(2.11) below

$$O_3 + Cl^- \leftrightarrow O_2 + ClO^- \quad (2.9)$$

$$ClO^- + O_3 \rightarrow Cl^- + 2O_2 \quad (2.10)$$

$$ClO^- + O_3 \rightarrow [\ldots] \rightarrow ClO_3^- \quad (2.11)$$

Considerable doubt is raised by the first reaction (2.9) proposed back in 1949 [70] and reported in many publications [71]–[73]. In order to elucidate its mechanism more precisely, Razumovskii reported the composition of the reaction products using the presence of strong absorption bands in the UV spectra of the most interesting reaction products, namely, toxic hypochlorite and chlorates, and by gravimetric method. The UV spectra of the expected products and the initial and ozonated solutions of NaCl are presented in **FIGURE 2.3**. No expected ClO^- and Cl^- were detected in the products but a new product, H_2O_2, appear.

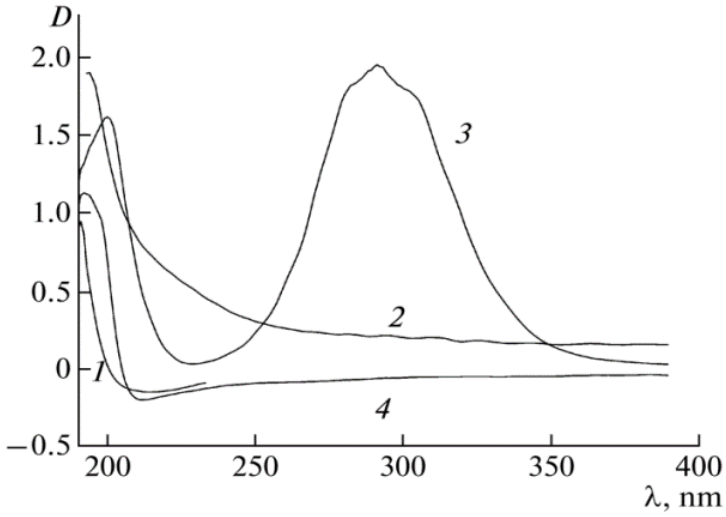

FIGURE 2.3 UV spectra of solutions: (1) initial solution of NaCl (0.9%); (2) hydrogen peroxide (0.2%); (3) sodium hypochlorite (0.2%); (4) difference between the absorbance of sodium chloride solutions before and after ozonation for 48 h (10% NaCl) [74].

Apart from the reactions (2.9) – (2.11) presented above, another version can be proposed for the mechanism of ozone decay as follows.

$$O_3 + Cl^- \leftrightarrow O_3^- + Cl^* \quad (2.12)$$

$$Cl^* + O_3 \rightarrow ClO + O_2 \quad (2.13)$$

$$ClO + O_3 \rightarrow Cl^* + 2O_2 \quad (2.14)$$

$$Cl^* + Cl^- \leftrightarrow Cl_2^- \quad (2.15)$$

The chlorine radical thus formed can further either rapidly add to Cl^- or attack the next ozone molecule by reaction (2.13). The complex radical ion can be regarded as a reservoir for accumulation of chlorine atoms. Reactions (2.9)–(2.11) are usually considered as the major channel of ozone decomposition [71][73]. This is based on a publication [69] which found that the hypochlorite ion ClO^- is easily oxidized by ozone (k = 120 L/(mol s)) to give Cl and to recover Cl^- (70%). Razumovskii verified the final reaction product, chlorate ion, is absent in the solution after completion of the reaction [75]. That was indicated by examinative the UV spectra and the weighing data for the dry residue obtained by distilling off water from the initial and ozonated salt solutions. The presumptive reaction products, ClO^- and Cl^- exhibit intense absorption bands in the UV spectra (**FIGURE 2.3**) (the positions of the peaks are at 292 nm, and 197 nm) [76]. Analysis of the UV spectra of solutions after long term bubbling of ozone (**FIGURE 2.3**) showed the absence of both Cl and intermediate ClO^-.

Hence, reactions (2.12) – (2.14) appear most likely and are accepted by many studies. This is supported by the direct detection of elemental chlorine in the system [68] and the absence of higher oxygenated chlorine salts in the reaction products. Previously, similar single electron transfer steps were found for the reactions of hydroxyl and phenoxide ions with ozone in solutions [77], [78]. The ozonide ion formed together with Cl^* is converted to O_2 and H_2O_2 by a known mechanism [78]. The fact that the electron affinity of O_3 is lower than that of Cl does not prevent the reaction but affects the equilibrium concentrations in the right hand and the left hand of reaction (2.12). Thermodynamic approach can be used to roughly estimate the Cl^* concentration in the solution.

The product of reaction (2.13) is chlorine monoxide ClO. It is a rather reactive molecule able to participate in many reactions, in particular, to react with ozone (2.14) [79]. Participation of ClO in ozone decomposition adequately interprets the absence of the products of deep oxidation of chloride ions. The presence of elemental chlorine in the system was proved in an experiment [68] where chlorine was blown off by air.

2.6 Disinfection methods for waste water

After the treatment of urban sewage, the water quality is significantly improved and the bacteria content is also greatly reduced. However, the absolute number of bacteria is still

considerably high. They must be removed before the wastewater can be safely discharged or recycled. With the continuous improvement of the quality of life of residents, the impact of secondary effluent from sewage treatment plants on the urban water bodies has attracted more attention for health and safety concerns. Disinfection is one of the basic methods of inactivating these pathogenic organisms. Therefore, the tail water disinfection of sewage treatment works has become an important process in sewage treatment.

Nowadays the disinfection technology utilizes three common methods chlorination ultraviolet irradiation and ozonation.

(1) Chlorination

Chlorination is the most commonly used disinfection method in water treatment and drinking water distribution, owing to its cost-effectiveness, simplicity, and systematic usage.

Chlorination disinfection method is to add liquid chlorine or hypochlorite (such as NaOCl) solution disinfection into water. The chemical reactions are as follows:

$$Cl_2 + H_2O \Leftrightarrow HOCl + H^+ + Cl^- \quad (2.16)$$

$$OCl^- + H_2O \Leftrightarrow HOCl + OH^- \quad (2.17)$$

In the above reaction, HOCl and OCl^- are the effective radicals, and HOCl has higher effectiveness for disinfection.

However, undesirable disinfection byproducts (DBPs) of the chlorination are known to be toxic and associated with reproduction and carcinogenic risk in humans, such as trihalomethanes, halogenated acetic acids, and halogenated aceto-nitriles [80]–[82]. Owing to the serious safety concerns, the chlorination disinfection because less popular [83].

(2) Ultraviolet radiation (UV)

UV irradiation is now the most common alternative to chlorination for wastewater disinfection in North America [84] . Nucleic acids (such as DNA and RNA) absorb energy of light in which, 240–260 nm, which can be emitted by UV lamps. The mechanism of UV disinfection is that adjacent thymine bases on the nucleic acid strands are dimerized when they are exposed to UV light. This prevents the accurate transcription of this DNA strand, and thus suppresses the division of the bacteria cell cannot divide [85].

Early studies [86] found that the UV dosage of 35 mJ/cm^2 is required to achieve a 3-log or greater reduction in fractional counts (FC). This shows the dosage could meet a goal level of 2000 CFU/100 mL before the dilution and the further photoreactivation. More recent studies [87] determined that doseage of 8–12 mJ/cm^2 could achieve a goal level of 1000 CFU/100 mL for suspended solids (SS) of 20–30 mg/L.

Many studies have been reported on the effect of UV on different microorganisms,

such as Angehrn [85], Masschelein [88] and Oppenheimer et al. [89]. The typical indicator aerobic bacteria show a relatively low resistance (e.g. a 1-log inactivation require approximately 2.5–3 mJ/cm^2), bacteriophages and many viruses are slightly more resistive, and the anaerobic spore-formers such as clostridium perfringens are the most resistive (over 10 mJ/cm^2 per log inactivation).

(3) Ozonation

Due to the difficultly of ozone generation and the requirement of high ozone concentration ozonation is not common in wastewater disinfection. But ozone has been a popular and successful disinfectant for drinking water. [90], [91] There are many researchers studied the kinetics of ozone reactions. However, different chemicals has different reaction rates in solution, the dissolved ozone have various decomposition products, which interact with the microorganisms in different ways. These make the kinetics of ozone reactions complicated. Based on the literatures, ozone decomposition can be separated into three phases, though some disagreement exists regarding the exact pathways [84]. The type and dynamics of ozone decomposition have strong implications on the disinfection mechanism. If the decomposition of ozone is slow, then the chemical substances would suffer direct ozone attacks. These reactions are selective and slow. On the opposite, if ozone decomposition is rapid, then OH^- radical would be produced by

oxidation, which is very reactive and non-selective. Studies with E. coli have shown that these organisms undergo greater inactivation when the ozone residuals persist, rather than when ozone is rapidly decomposed.

The actual mode of ozone disinfection is still poorly understood. Some researchers claimed that ozone changes the proteins and the unsaturated bonds of fatty acids in the cell membrane, or that it affects the cell DNA. Hunt and Marinas [92] showed that noticeable changes in the interior of E. coli cells did not take place until most of the cells in the sample were non-viable. This confirms the hypothesis that in most cases the inactivation is due to the damage of the cell membrane. The DNA damage might still occur, but only if ozone dosage is very high.

The three disinfection methods are summarized in **TABLE 2. 2**. Important aspects are discussed, including the reaction time, the effectiveness in killing bacteria and viruses, the cost issues, the advantages and the disadvantages. Generally speaking, chlorination is the oldest method in disinfection and causes the secondary pollution, whereas the other two methods have different pros and cons.

TABLE 2. 2 Comparison of different disinfection method.

	Chlorination ($HOCl$, OCl^-)	Ultraviolet radiation (UV)	Ozone (O_3)
Reaction time	10-30 minutes	<1 second	5-10 minutes
Effectiveness of killing bacteria	Yes	Yes	Yes
Effectiveness of killing virus	Partly	Partly	Yes
Cost of equipment	Lowest	Highest	5 times higher than Chlorination
Cost for running	Lowest	Higher than chlorination, similar to ozone	Higher than chlorination, similar to UV
Advantage	1. Cheap 2. Mature 3. Continuous sterilization	1. Fastest disinfection method 2. No secondary pollution	1. Broad-spectrum sterilization 2. No secondary pollution
Disadvantages	1. Invalid to virus 2. Its oxidation is harmful to humans 3. Irritating smell and damage human skin	1. Expensive 2. Cannot continuous sterilization 3. Have water pretreatment requirements 4. Weak penetration	1. Expensive 2. Cannot continuous sterilization 3. High safety requirements

2.7 Summary

This chapter has reviewed several important aspects of waste water treatment, including the principle of photocatalysis, the photocatalytic semiconductor materials, the fabrication methods of photocatalyst films, the common designs of photocatalytic reactors, the influence of salt ions, the ozonation process and the common disinfection methods. These provide the technical bases for the detailed experiment studies on new photocatalytic reactors for decontamination of waste fresh water in Chapter 3, new photocatalytic ozonation of sea water in Chapter 4 and new UV-ozone combined method for complete disinfection of waste water effluents in Chapter 5.

CHAPTER 3. PLANER SOLAR REACTORS FOR PHOTOCATALYTIC PURIFICATION OF FRESH WASTE WATER

Many types of solar reactor have been developed for photocatalytic degradation of organic pollutants in waste fresh water, but they often have some defects, such as open chamber or using suspended photocatalyst, which causes the leakage of pollutants or the difficulty to collect the photocatalyst after the treatment. To avoids these problems, this study will propose a planer reactor with a closed chamber and a photocatalyst film, which has large light-receiving area and fine control of the flow properties. Using the same reactor design, a small chip-size reactor and a large-size reactor are fabricated, the former is for laboratory test and the latter is for exploring industrial application. In this chapter, the design, the fabrication and the experimental results will be presented.

3.1 Design of planer reactor

The design of the clip-size reactor and large-size reactor is the same, as shown in **FIGURE 3.1**. It has a square reaction chamber, which is constructed from a nano-porous TiO_2-coated film as the cover and the substrate and a 100-μm-thick PDMS layer as the

spacer and sealant. In the planar reactor, the TiO_2 films ha the same surface area as the reaction chamber, making the best use of the surface area for light receiving and photocatalytic reaction.

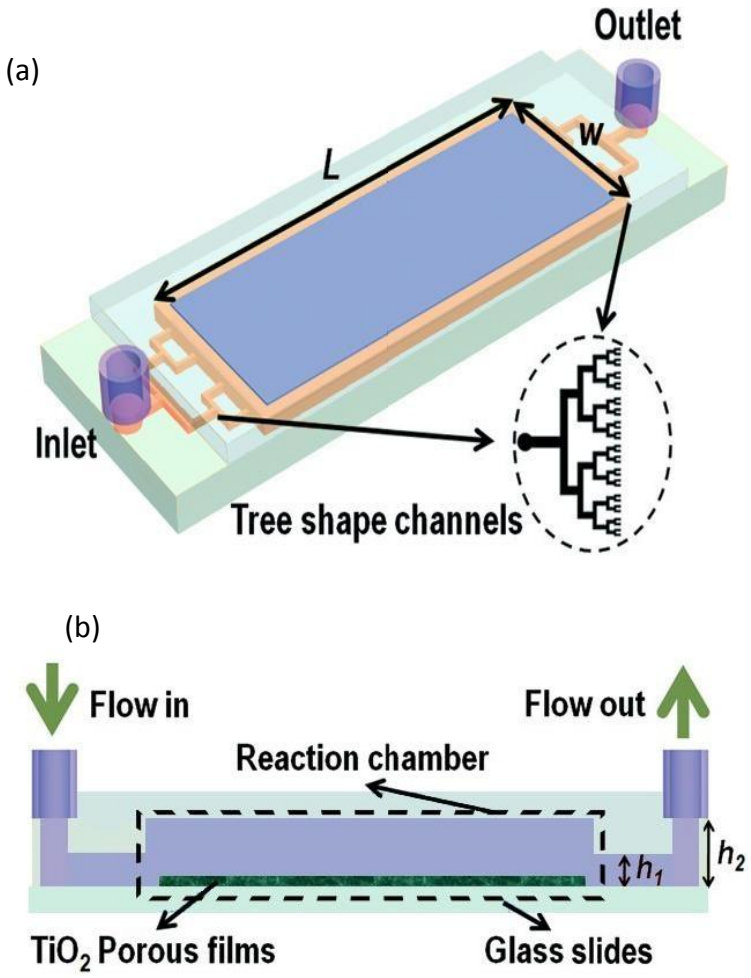

FIGURE 3.1 (a) Schematic view and (b) Cross-sectional view of the planer reactor.

In the chip-size (called microreactor), the liquid layer is 100 μm thick, and thus the nominal surface area to volume ratio (SA:V) of the microreactor is SA:V = $1/h_2$ = 10 000 m^{-1}, where h_2 is the height of reaction chamber (see **FIGURE 3.1**(b)). As compared to the micro-reactor, the large-size reactor has a rectangle reaction chamber, which also uses a nano-porous TiO_2-coated film as the cover and the substrate but a 1-mm thick PMMA layer as the spacer and sealant. In that device, the nominal SA:V is 1000 m^{-1}.

3.2 Design of photocatalytic films

Based on the literature review, the spray pyrolysis method is found to be the best way to make the thin film since itis the simplest method, and allows continuous production. In the clip-size reactor. Since it is easy to deposit TiO_2 film. However, the substrate for the large-size reactor cannot be glass due to the brittleness. The common nonbrittle materials are metal and plastic. Since the photocatalysis contain oxide-reduction reactions, metal is not a suitable material for the substrate. In contract, PMMA is more suitable for the substrate of the large-size reactor, since PMMA is cheap, nonbrittle, lightweight, transparent in UV light and easy for machining. In addition, PMMA has good UV transmission spectra. The transmission spectra of glass and PMMA are showed in **FIGURE 3.2**. It is seen that the cut-off wavelength is 360 nm for glass and 300 nm for

PMMA. Therefore, the use of PMMA as the cover and the substrate allows for better utilization of sunlight is the UV range.

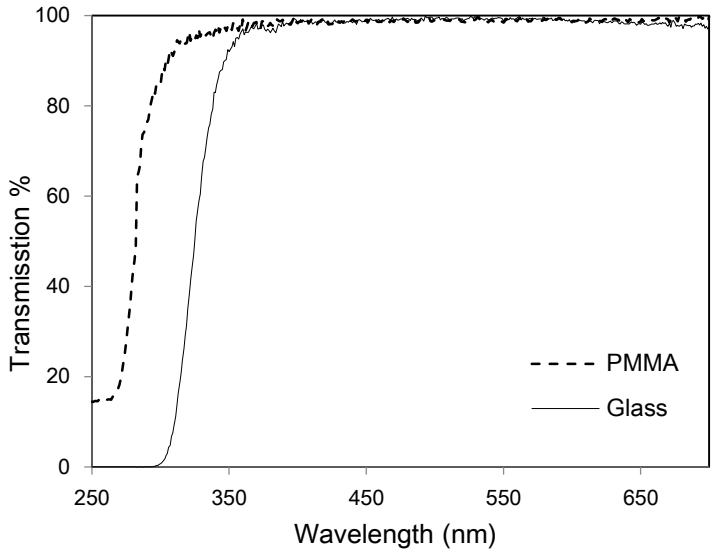

FIGURE 3.2 Absorption spectrum of PMMA and glass.

However, PMMA cannot sustain 150℃ since it would be melted. Therefore, any high-temperature methods like pyrolysis or thermal annealing cannot be used in the fabrication of the photocatalyst film of the large-size reactor. In this study, we develop a new fabricate method soaking-spray method which is similar to the spray pyrolysis method, except for the step to fix photocatalyst powder onto the substrate.

3.3 Fabrication procedures of photocatalytic films

The fabrication procedure of photocatalytic film can be divided into three steps, surface handling, spraying and fixing. But they are different for the chip-size reactor and the large-size reactor.

3.3.1 Chip-size reactor

The chip-size reactor uses a glass slide as the substrate. The procedures are as follows:

(1) Surface handling

The substrate of clip size photocatalytic film is glass; it was washed by ultrasound cleaning 80 W for 15 minutes with acetone firstly, repeat the washing step by switching acetone to absolute ethanol, leaving power and time unchanged. Finally switch ethanol to DI water and redo the washing.

(2) Spraying

After the cleaning produce, the substrate can move to spraying produce. Firstly, the TiO_2 solution was prepared. The formulas for clip size and large scale are different. The TiO_2 solution mixing by 60 mL DI water, 0.75mL Triton X-100, 1.5mL Acetylacetone and 5 g TiO_2 P25 powder and stirring 24 hours is for clip size.

And then the solution was put into the gas tank and was injected the pipe into the

solution. The compressed air was injected into the gas tank and the air pressure was adjusted until the reading of the pressure meter on the tank reaches 5bar, and the air pressure valve was adjusted on the panel of the controller to 4.2bar. The amount of TiO_2 sprayed out was adjusted by rotating the rotary knob on top of the sprayer. And then the suitable programe was selected and the teaching mode of the dispenser, the important parameters including start point and end point of each linear spraying, height of the sprayer and moving speed of the sprayer. And then the TiO_2 particular was spray on the substrate prepared.

(3) Fixing

After the film was built on the substrate, the film would fall down easily, so the film needs to fix on the substrate. The clip size film would heat up to 500^{o}C 10 hour for fixing the film.

3.3.2 Large-size reactor

The large-size reactor uses a PMMA plate as the substrate. The procedures are as follows:

(1) Surface handling

Different substrate is using different cleaning method to clean, since acetone would corrosion the surface of PMMA and the large size film is too large so ultrasound

cleaning is not suitable.

The substrate of large scale photocatalytic film is PMMA. It would clean by hand wash with detergent. And the PMMA was soaking into dopamine 2.5mg/mL with 0.1M HCl buffer 24hour for changing the surface to hydrophilic.

(2) Spraying

The spraying process for large-size reactor is similar to the process for chip-size reactor. But the large-size reactor would not be heat up. So the TiO_2 solution for large size film would not added Triton X-100, and Acetylacetone.

(3) Fixing

The large-size film would be soaking into chloroform 1 second for corrosion the surface. After the chloroform volatilized, the film would be fixed on the PMMA.

3.4 Fabrication procedures of reactors

The chip-size reactor was made by modeling method. And large-size reactor was made by combination method.

3.4.1 Chip-size reactor

The modeling method for making micro-reactor was used silicon wafer for the support.

The silicon wafer was washed by ultrasound cleaning 80W 15minutes with acetone firstly, repeat the washing step by switching acetone to absolute ethanol, leaving power and time unchanged. Finally switch ethanol to DI water and redo the washing. And then SU-8 negative photoresist was put onto the wafer and was spin 5000rpm with 2 minute, and then was explored by UV light with pattern protection. After that, the wafer with pattern was soaked into developer to develop the pattern. And the modeling was created.

The silicone elastomer (PDMS) was mixed by 10: 1 hardener. The PDMS was put onto the wafer with pattern and heat-up to 65^{o}C for 15 minutes for solidify. And the model of the micro-reactor was removed from the wafer.

And then the model of the micro-reactor and the substrate with photocatalytic film were put into oxide plasma machine to combine them.

3.4.2 Large-size reactor

The large-size reactor was made by simple combination method since that is suitable for industry mass production. The transparent PMMA cover, black PMMA support sheet and black PMMA roll were combined by polymerized siloxanes and screws.

3.5 Calibration of photodegradation

In the photocatalytic experiment, methylene blue (MB) is used as the model chemical.

The change of MB concentration before and after the photodegradation reflects directly the efficiency of photocatalysis. Here the MB concentration is measured by UV-vis spectrophotometer. Before the tests of photocatalysis, a calibration is conducted to find the relationship between the absorption and the concentration of MB have been done.

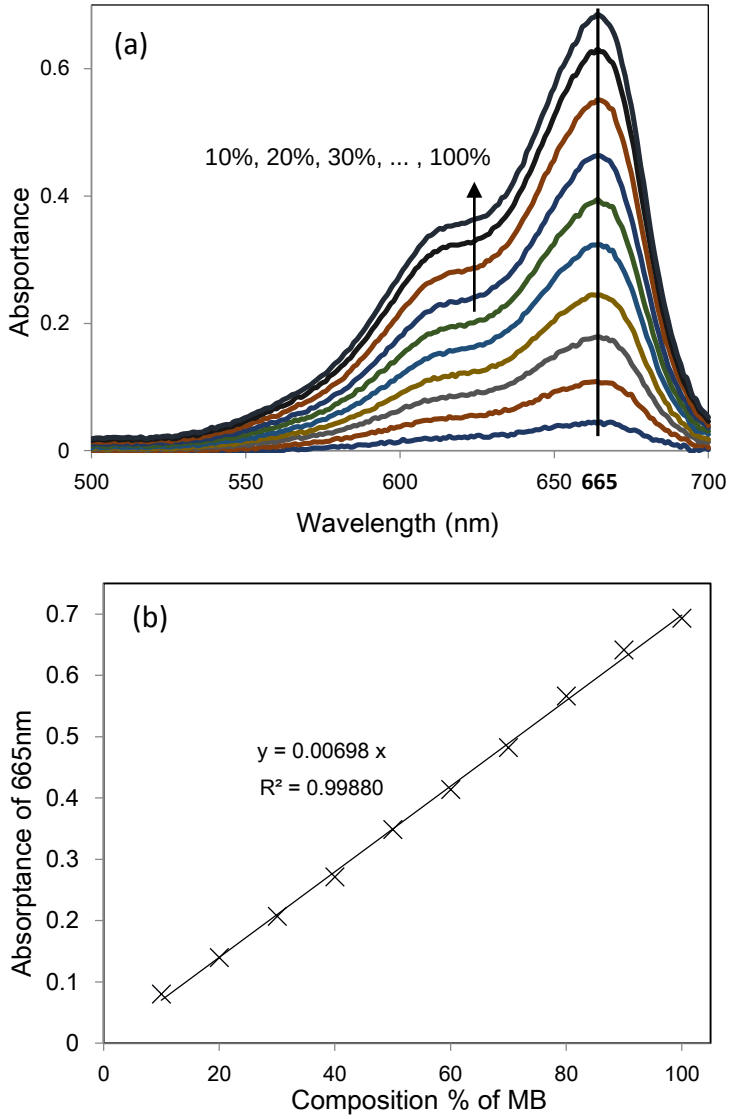

FIGURE 3.3 Calibration of MB concentration. (a) Absorption spectra of MB solutions. (b) The absorptance of 665 nm as a function of MB concentration.

The standard MB solution is set to be 3×10^{-6} M. Then 10%, 20%, 30%, ... , 100% samples are prepared by mixing the standard solution with DI water.

As shown in **FIGURE 3.3 (a)**, the absorption spectrum lifts up with the increase of MB concentration. It is also observed that there is an absorption peak at 665 nm, while can be used to track the MB concentration change. The absorptance of 665nm is proportional to the concentration of MB as plotted in **FIGURE 3.3 (b)**, the linear fit gives y = 0.00698x, in which y is the absorptance and x is the percentage of the standard MB solution (3×10^{-6} M). With this, the MB concentration and thus the photocatalytic efficiency can be determined easily.

3.6 Experimental results

In this study, a chip-size reactor and a large-size reactor are fabricated, whose photocatalytic TiO_2 thin films are made by different methods. These two reactors are tested separately. The results are stated below.

3.6.1 Chip-size reactor

FIGURE 3.4 shows SEMs images of TiO_2 film in the clip-size reactor. Based on the work by Zhang[93], the continuous film has higher efficiency to degrade organics. **FIGURE 3.5** shows the absorption spectrum of the TiO_2 film, which has an absorption peak at 344

nm. According to the work by Mohammad [94], the energy band gap of TiO_2 is 3.15eV and the absorption would start at 393 nm. The difference is due to the absorption of the glass subtraction, which adds up to the total absorption.

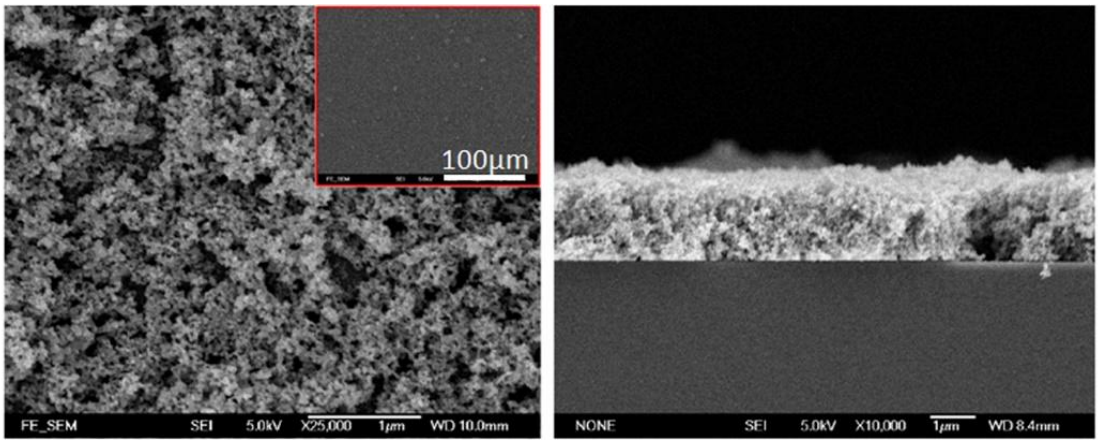

FIGURE 3.4 SEM images of TiO2 film in the clip-size reactor.

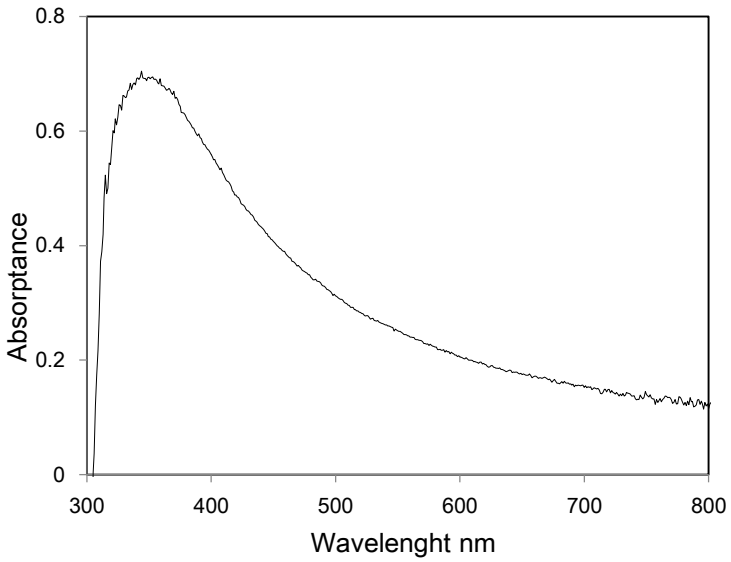

FIGURE 3.5 Absorption spectrum of the TiO_2 film of the chip-size reactor.

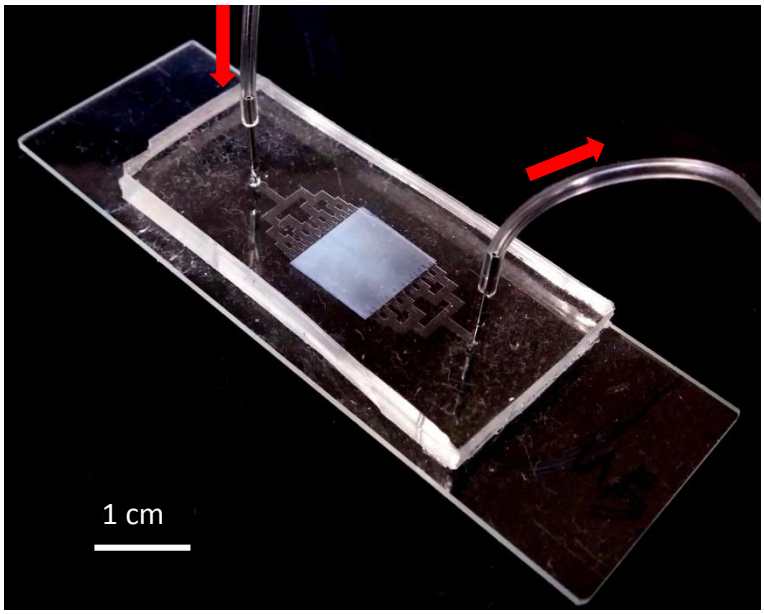

FIGURE 3.6 Experiment device of the clip-size reactor.

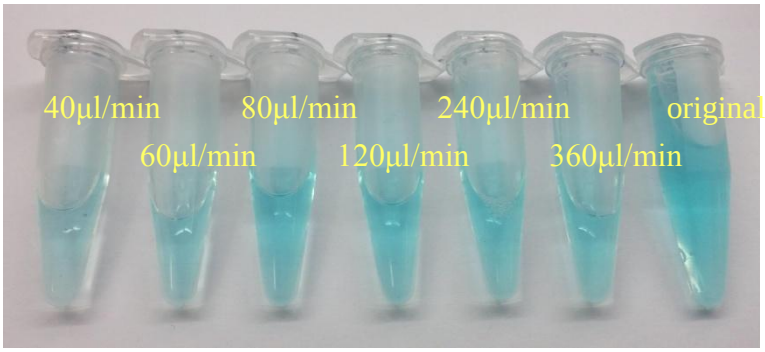

FIGURE 3.7 Color change of the MB solution after photocatalysis with different flow rates in the clip-size reactor.

FIGURE 3.6 shows the optical image of the chip-size reactor. The tree-shaped channels are used to make sure the water layer is flow of uniformly through to the photocatalytic chamber. The size of TiO_2 film is 1 cm × 1 cm. The inlet and the outlet are

connected to an external syringe pump to control the flow rate of the MB solution.

The first test is operated under normal condition (including UV light and TiO_2 film). **FIGURE 3.7** shows the colours of MB solutions at the flow rates of 40, 60, 80, 120, 240 and 360 μl/min (from left to right), corresponding to the residence times (i.e. reaction time in the chamber) of 150s, 100s, 75s, 50s, 25s and 16.67s, respectively. The first one on the right side is the original MB solution for reference. The colour becomes lighter and lighter from right to left, indicating better degradation of MB at lower flow rate.

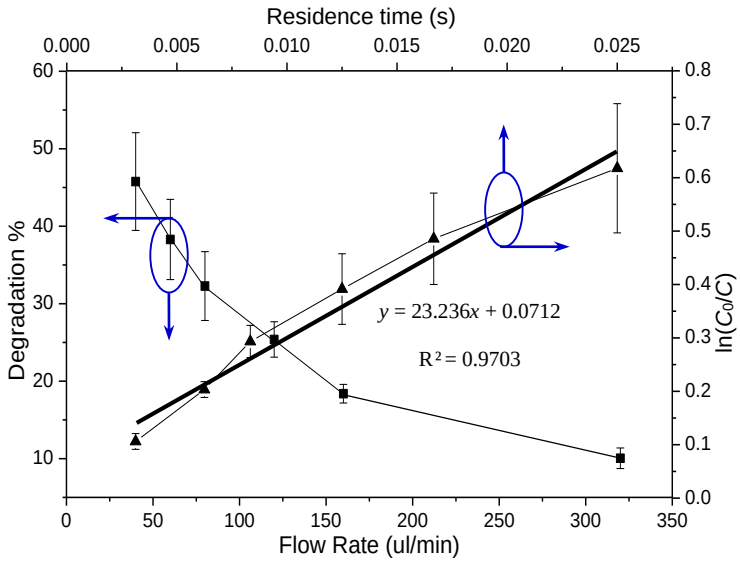

FIGURE 3.8 The relationship between the degradation % and the flow rate. The upper and the right areas show the relationship between the degradation exponent $\ln(C_0/C)$ and the residence time.

FIGURE 3.8 shows two relationships in one diagram. The first is the degradation

percentage and the flow rate, which shows an exponential decrease. And the second is between ln(C_0/C) and the reciprocal of flow rate, which shows a linear relationship. The error bar is due to the variation of water flow. A slow velocity of water flow increases the irradiation time, heats up the solution, decreases the solubility of oxygen in water, and increases of the error range. In all the tests, a solar simulator of 303 W is used as the light source.

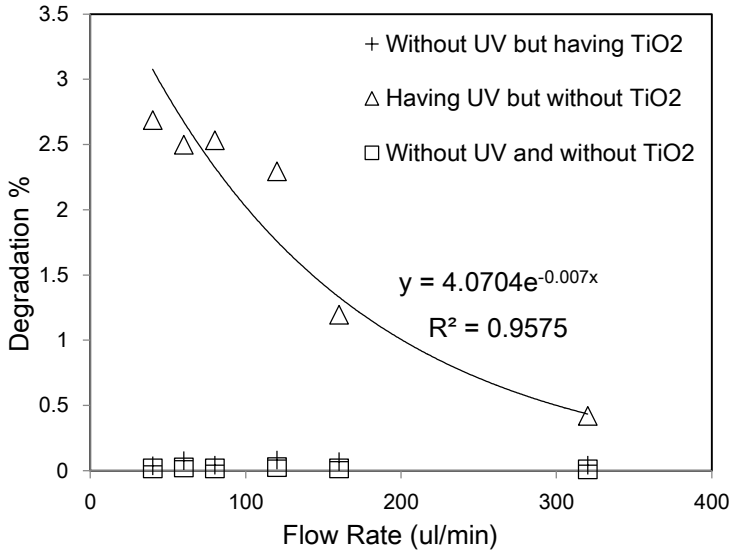

FIGURE 3.9 The degradation % in control experiments.

The following experiments have a serial of control experiment, including the chamber without TiO_2, the operation under non-UV light and the test of self degradation (i.e. photolysis). **FIGURE 3.9** shows the degradation percentage in three control

experiments. The first control experiment is the reactor under the irradiation of UV-fitter sunlight. The results show less than 0.1% degradation. The second control experiment is an empty reactor (without TiO_2 film) under the simulated sunlight. The results show less than 3% degradation, which is due to the self-degradation of MB. In the third control experiment, the reactor has no TiO_2 film and the simulated sunlight is filtered out the UV part. The results are <0.1%, showing that the photolysis of MB by visible light is negligible.

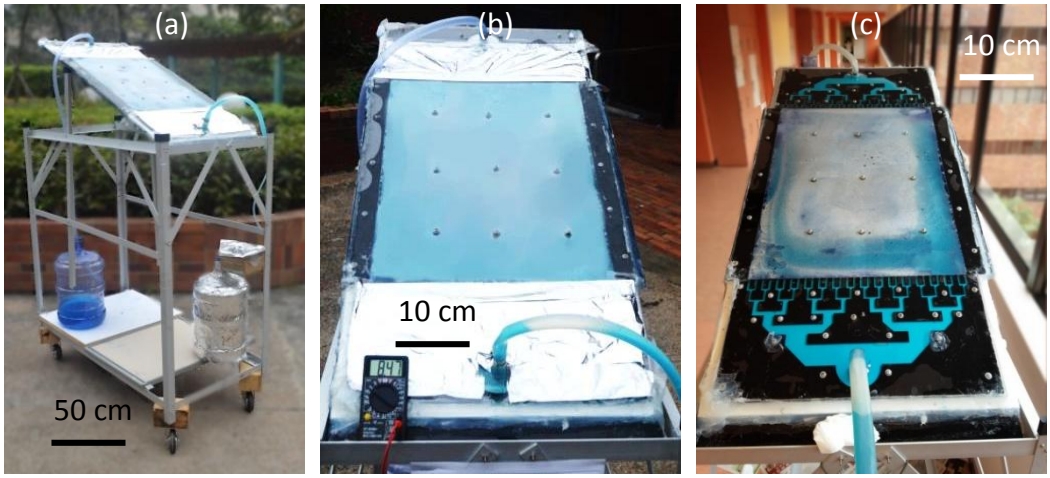

FIGURE 3.10 Photos of the large-size reactor system. (a) The whole system and the reaction chamber region; (b) with adding the surfactant to the MB solution and (c) without adding the surfactant to the MB solution.

3.6.2 Large-size reactor

FIGURE 3.10 shows the photos of the large-size reactor operated in outdoor sun light. The structure of the large-size reactor is the same as that of the chip-size reactor. However, the size of photocatalytic film is scaled up to 60 cm × 40 cm. The reactor is inclined at 23° above horizontal surface since the altitude of sun in Hong Kong is 23°. The flow rate is set at 18 mL/min, as compared to only 158.8 μL/min in the chip-size reactor. The original MB solution (see **FIGURE 3.10 (a)and(b)**) is stored in the bottle shielded by aluminum foil. In **FIGURE 3.10 (a)**, the MB solution is added with surfactant, but in **FIGURE 3.10 (c)** it is not. The surfactant is coconut oil alchol surfactant with 27.7 μL/L concentration. It is to reduce the influence of the hydrophobic problem and common used in making soap. Since the PMMA is a hydrophobic material, some MB solution is trapped inside the reactor chamber. This would affect the uniformity of the flow in the reaction chamber and reduces the photodegradation efficiency.

FIGURE 3.11 shows the colour change of the thin film in different fabrication steps. The original PMMA plate is black. After the soaking-spray of TiO_2 P25 powders (80% anatase, 20% rutile), it changes to light gray, showing the successful formation of a TiO_2 film. After the ultrasound treatment, the film color become slightly dark, inciting the

removed of loosely-fixed TiO_2 powders. This ensures the TiO_2 film can work stably over long operation time.

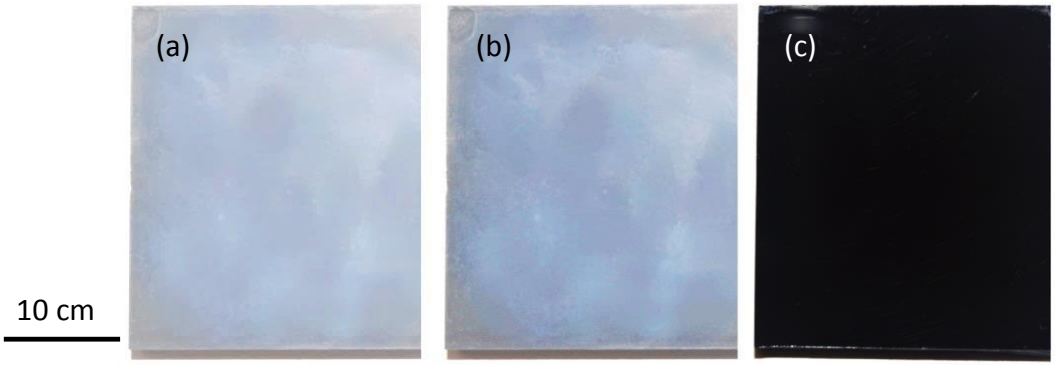

FIGURE 3.11 (a) The fabricated thin film; (b)the thin film after the ultrasound treatment; and (c) original PMMA plate.

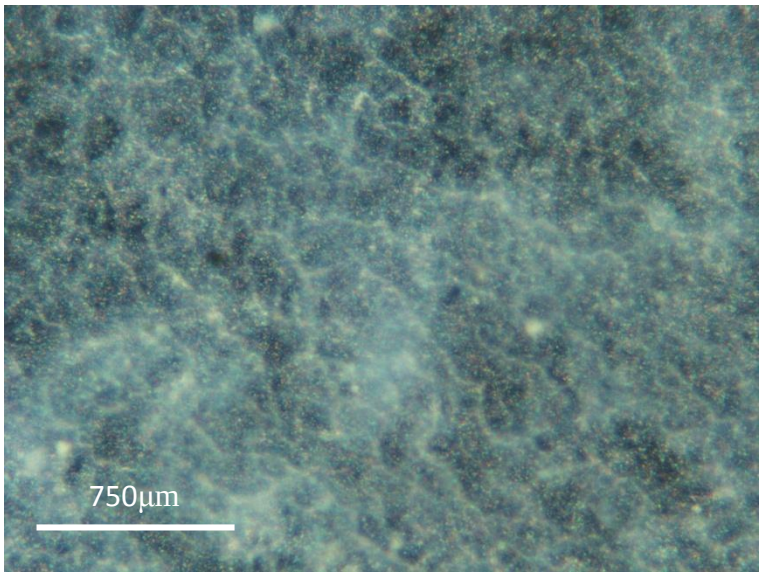

FIGURE 3.12 Close-up of the TiO_2 film in the large-size reactor.

FIGURE 3.12 shows the enlarged view of the TiO_2 film in the large-size reactor. Although the film continuity is not as good as that of the structure in the clip-size reactor,

the process is simple and easy to make large films.

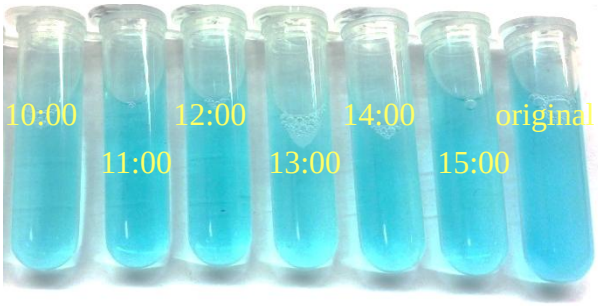

FIGURE 3.13 Color change of the MB solution after the photodegradation for 2 hours. Starting from different times of a sunny day using the large-size reactor.

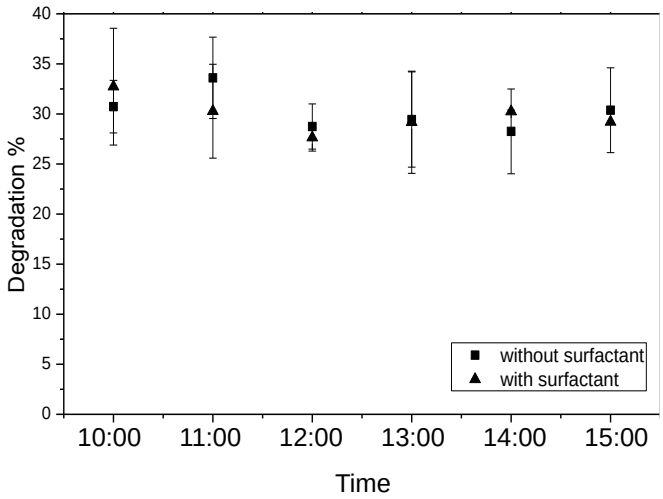

FIGURE 3.14 The relationship between the degradation % at the starting time of 2 hours operation in outdoor sunlight.

FIGURE 3.13 shows the colours of MB solutions when the large-size reactor is operated for 2 hours under sun light outdoors starting from 10:00, 11:00, 12:00, 13:00, 14:00 and 15:00 (from left two to right two). The rightest one is the original MB solution

for reference, and the leftest one is the MB solution in sun light for 2hours without the TiO_2 film. The latter is due to the photolysis and it only 1.27%.

FIGURE 3.14 shows the degradation percentage of MB as a function of the start time of operation under sun light outdoor. The flow rate is maintained at 18 ml/min, corresponding to a reaction at 2 hours. The experimental data (square points) show that the degradation is about 30%, each point is a result of five tests. The error bar is due to the variation of sunlight over different days. Although the degradation of 30% over 2 hours is not very satisfactory, it is already 23.6 times of the photolysis (i.e. 1.27% for 2 hours) To avoid the hydrophobic problem, surfactant has been added. However the degradation percentage does not increase significantly. One of the reasons is that the degradation efficiency of MB is affected by the surfactant.

3.7 Summary

This chapter has proposed a new planner design of the photocatalytic reactor, which enables fine control of water flow and large light receiving area. Using the same design but different substrate materials and fabrication methods, a chip-size reactor and a large-size reactor have been developed. The former is for laboratory test and mechanism study, whereas the latter is the explore the feasibility to process large volume of waste water to

prove its way to real industrial applications. Experimental tests show a degradation of 30% of MB when the reaction is operation for 2 hours in outdoor sunlight. Although the efficiency is not high, it is already 23.6 times of the photolysis, and the use of sunlight is abundant, environment friendly. To degrade the organic pollutants at much faster pace, we need to introduce other more powerful method like UV-based photocatalysis and ozonation. This will be presented in next chapter.

CHAPTER 4. PHOTOCATALYTIC OZONATION OF SEAWATER

The previous chapter has developed a large-scale solar reactor for purification of polluted freshwater using photocatalysis. However, the photocatalysis is often not effective in seawater decontamination due to the existence of salt ions, which severely affect the chemical reactions of oxidation and reduction in photocatalysis. For this reason, the seawater decontamination is usually not practical if it relies on only the photocatalysis. To avoid this problem, this chapter will combine the photocatalysis and the ozonation to decontamination the polluted seawater with high efficiency and low cost. This is the first study of photocatalytic ozonation of seawater and this work is thus original and novel.

4.1 Experimental setup

Decontamination experiment is carried out using a reactor system as shown in **FIGURE 4.1**. The UV reactor consists of a cylindrical container (height 20 cm and inner diameter 9 cm), a UV light source and an ozone supply system. The cylindrical container is filled with the water sample. The UV light source is a medium pressure Hg tube (25 W with 8 W in the UV-C spectrum, from Cnlight Ltd). It is inserted along the central line of the

container to irradiate the water sample. The ozone supply system utilizes compressor air as the gas source. Part of the compressed air (CA) goes through an ozone generator (OG, from YEK High-Tech Ltd.) to generate ozone gas by electric discharge. The other part of compressed air is monitored by a flow meter (FM1) and is then used to dilute the ozone gas via a gas mixer (GM). An ozone sensor (OS, from Bosean) is used to monitor the ozone concentration and another flow meter (FM2) is used to measure the flow rate of mixed ozone gas. The ozone concentration can be controlled by adjusting the flow rate of the diluting compressed air. Finally, the ozone gas is pumped into the bottom of the cylindrical container. Two aeration stones (length 27 mm and diameter 12 mm) are used to disperse the ozone gas into small bubbles. This improves the dissolution of ozone into water and helps stir the water sample when the bubbles move up.

In the decontamination experiments, if only the ozonation effect is tested, the photocatalyst and the UV tube are not placed in the cylindrical container. For the photocatalysis and/or the UV effect, the photocatalyst and/or the UV tube will be used correspondingly. After the degradation process, the water sample is measured by a UV-visible spectrometer (UV-2550, spectral range 250 – 900 nm, from Shimadzu).

To indicate the degradation, the model chemical utilizes the dye solution of methylene blue (MB) with the concentration of 3×10^{-5} M. The sea water sample is

artificial sea water which contains 35wt% sea salt, corresponding to the NaCl concentration of 0.6 M. The photocatalytic material is P25 TiO_2 nanopowder (Aeroxide, Sigma Aldrich) with the primary particle size of 21 nm. The TiO_2 solution has the concentration of 1 g/L.

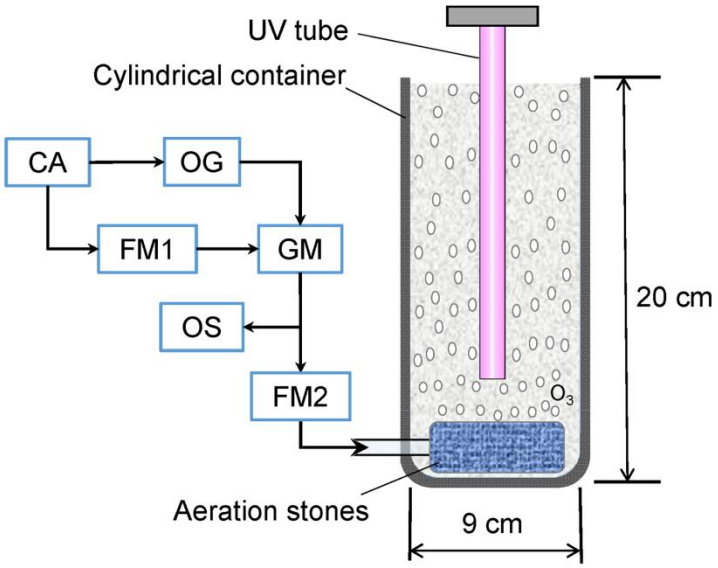

FIGURE 4.1 Schematic diagram of the experimental setup. The cylindrical reactor contains the water sample and has a UV tube inserted at the center as the light source. The bottom of the reactor has aeration stones for dispersing the pumped gas into bubbles. The concentration of ozone is controlled by mixing the compressed air with the ozone from an ozone generator. CA: compressed air source; OG: ozonation generator; FM1: flow meter 1; GM: gas mixer; OS: ozone sensor; FM2: flow meter 2.

4.2 Experiment process

The experimental study consists of serval parts, the study of ozone solubility, the comparison of decontamination powers of ozone and photocatalysis, the synergistic effect

of photocatalytic ozonation and the influences of salt in photocatalytic ozonation. The experimental procedures are described as below.

(1) The solubility of ozone in SW and DIW

DI water (18.2MΩ) and artificial sea water are used. Different concentrations of ozone are pumped into the solution by the reactor. To measure the ozone concentration using colorimetry overdose potassium iodide (KI) is used to reduce iodine, and then starch is added to change the color from colorless to dark-blue. Another test of the iodine concentration in water is also conducted for calibration. Second this test, different concentrations of iodine are added in to 5% ethanol solution before adding starch, and the color of the dark-blue solution is measured by UV-vis-spectrometer. According to Jacek Majewski's work, the detection limit is 75 ppbw (equal to 75 μg/L) [95].

(2) Ozone oxidation in different concentrations of ozone

30 μM MB solution in SW is pumped in different concentrations of ozone. And the colour change is measured by UV-vis spectrometer.

(3) PCO in different concentrations of ozone

The procedure is similar to the pervious part. However, 1 g/L TiO_2 P25 nanoparticle is dispersed into the solution. And the UV source is provided during the reaction.

(4) Synergistic effect of PCO

Photocatalysis degradation in SW with 30-μM MB solution is done for reference. And the degradation efficiencies of the photocatalysis, the PCO and the ozonation are compared to find out the synergistic effect of PCO.

(5) Degradation under different salt concentrations

25%, 50% and 75% artificial SWs with 30-μM MB solution are used to test the PCO effect. The procedure is similar to the PCO of different concentrations of ozone. Nevertheless, the concentration of ozone.

4.3 Mechanism of PCO for water treatment

For proper design of experiments and appropriate interpretation of test results in this work, the reaction mechanisms that underlie the photocatalysis, the ozonation and the PCO should be investigated. Many articles have reported detailed studies [1], [52], [96]. Here we will summarize those directly related to our work. **FIGURE 4.2 (a)** depicts the mechanism of photo-excited electrons and holes pair when the TiO_2 particle is irradiated by the photons with the energy ≥ 3.2 eV.[97] On the TiO_2 surface, the electrons and holes can be captured by the ions and other chemical species in the water sample. In the fresh water, the major compounds are H^+, OH^- and dissolved O_2. In the sea water, there are

abundant Cl^- ions. For instance, the concentration of Cl^- is 0.6 M in 3.5 wt% sea water. Therefore, the reaction pathways become different.

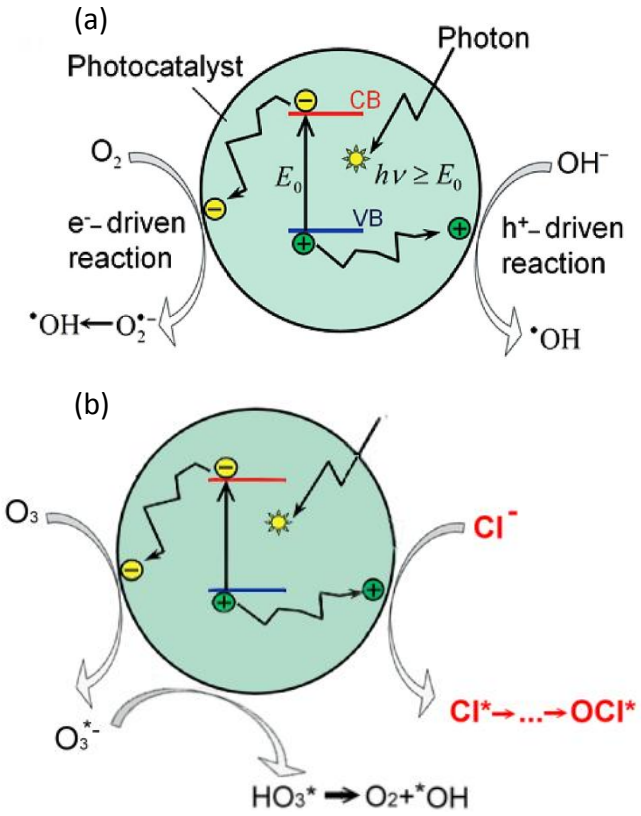

FIGURE 4.2 Mechanisms of the semiconductor photocatalysis in fresh water and the photocatalytic ozonation in sea water; (a) In the photocatalysis of fresh water, the photo-excited electrons and holes react with dissolved O_2 and OH^- to generate free $^*OH$ radicals, which has high oxidation power to oxidized most organic pollutants; (b) In the photocatalytic ozonation of sea water, the electrons are captured by O_3 to generate $^*OH$, and the holes are scavenged by Cl^- ions to generate OCl^* radicals.

For the photocatalysis in the fresh water, the holes can directly oxidize the organic pollutants or combine with OH^- to form $^*OH$ radicals, which are highly oxidative; and the electrons can be scavenged by the adsorbed O_2 molecules, which eventually form $^*OH$ radicals for oxidation of the organic pollutants.[1], [52], [96] However, in the sea water, the photocatalytic reactions are very different, as illustrated in **FIGURE 4.2 (b)**. In this case, the direct hole oxidation is prohibited. Instead, the holes are scavenged by the abundant Cl^- ions to convert into the Cl^* radicals and the OCl^* radicals, which are all oxidative.[98]–[101] Now we can see that the major oxidative species are the Cl^* radicals in the sea water, as compared to the $^*OH$ radicals in the fresh water. Since Cl^* has weaker oxidation power than $^*OH$, the sea water has a weaker photocatalytic activity than the fresh water.[102][103]–[105] For easy discussion, the oxidation powers of some common agents are listed in **TABLE 4. 1** . For instance, the hydroxyl radical *OH has the redox potential of 2.86 V with respect to standard hydrogen electrode (SHE), just slightly lower than that of fluorine atom (2.87 V vs. SHE).

TABLE 4. 1 Redox potential of oxidizing agents with respect to standard hydrogen electrode (SHE) [71].

Species	Potential (V vs. SHE)
Fluorine atom (F)	2.87
Hydroxyl radical (*OH)	2.86
Oxygen atom (O)	2.42
Ozone molecule (O_3)	2.07
Hydrogen peroxide (H_2O_2)	1.78
Hypochlorous acid (HOCl)	1.49
Chlorine atom (Cl)	1.36
Chlorine dioxide (ClO_2)	1.27
Oxygen molecule (O_2)	1.23
Hydrogen atom (H)	0.00

The ozonation processes are also different in fresh water and sea water. In fresh water, the dissolved ozone molecules can directly oxidize the organic molecules, or combine with OH^- ions to form *OH radicals.[106], [107] In sea water, the ozone molecules can still contribute to the direction oxidizing reaction. Nevertheless, the abundance of salt ions like Cl^- makes it more probably go through indirect reactions to form ClO^- and ClO_3^- ions [70]–[72]. In the sea water, the oxidizing species are mainly ClO^-, which are different from *OH radicals in the fresh water. Since the oxidizing power of ClO^- (potential 1.49 V vs. SHE, see **TABLE 4. 1**) is weaker than that of *OH (potential 2.86 V vs. SHE), it is expected that the ozonation effect in sea water is weaker than that in fresh water.

Here we present more details of the mechanisms of PCO in fresh water and sea water.

In fresh water, the ozonation in the presence of UV-irradiated TiO_2 can produce $OH^{\bullet}$ radicals by forming an ozonide radical (O_3^{*-}, see **FIGURE 4.2 (b)**), [108],[109] which can go further to form the $^{*}OH$ radicals. The reactions are as below.

$$O_3 + e^- \rightarrow O_3^{*-} \quad (4.1)$$

$$O_3^{*-} + H^+ \rightarrow HO_3^{*} \quad (4.2)$$

$$HO_3^{*} \rightarrow O_2 + {}^{*}OH \quad (4.3)$$

In sea water, the Cl^- ions can react with the already-generated oxidizing radicals (e.g., HO_3^{*}, $^{*}OH$) by possible reactions like (see **FIGURE 4.2 (b)**)

$$HO_3^{*} + Cl^- \rightarrow Cl^{*} + OH^- + O_2 \quad (4.4)$$

$$^{*}OH + Cl^- \rightarrow OCl^{*-} + H_2O \quad (4.5)$$

$$OCl^{*-} + H^+ \rightarrow HOCl \quad (4.6)$$

$$^{*}OH + ClO_3^- \rightarrow OH^- + {}^{*}ClO_3 \quad (4.7)$$

Again, the resulted ions Cl^{*}, OCl^{*-} and $^{*}ClO_3$ have weaker oxidizing powers. Therefore, the sea water has a weaker PCO effect than the fresh water.

Based on the above discussions of the mechanisms, we can summarize that: (i) the sea water has always weaker oxidizing effect than the fresh water in all the processes of the photocatalysis, the ozonation and the PCO, this is due to the reaction of salt ions (like Cl^-) with the highly oxidative radicals (e.g., $^{*}OH$) to generate relatively weak radicals (like OCl^{*}, $^{*}ClO_3$); (ii) the PCO has faster oxidation rate than only the photocatalysis or

only the ozonation due to the combined effect of the direction ozonation and the rapid scavenge of photo-excited electrons. However, the study of mechanisms cannot tell whether the photocatalysis and the ozonation have a synergistic effect (i.e., the PCO effect is higher than the summation of the photocatalytic effect and the ozonation). This needs experimental studies.

4.4 Results and discussion

4.4.1 Solubility of ozone in SW and DIW

Since the PCO combines the photocatalytic process and the ozonation process at the same time, the solubility of ozone in the solution would directly affect the performance of the organic degradation. Therefore, the solubility is first examined in this work.

In theory, Henry's law is the base for the study of gas solubility. It states that the amount of dissolved gas is proportional to its partial pressure in the gas phase. The proportionality factor is called the Henry's law constant H (i.e., the solubility), which is the ratio of the aqueous phase concentration c_a to its gas phase concentration c_g as given by $H = c_a/c_g$. For an ideal gas, the conversion can be transferred as $H = H^{cp} \times RT$, where $H^{cp} = c_a/p$, p is the partial pressure of that matter in the gas phase under equilibrium conditions, R is the gas constant and T is the temperature (in K). Sometimes, this

dimensionless constant is also called the "water-air partitioning coefficient" K_{WA}. It is closely related to the slightly different definitions of the “Ostwald coefficient”.[110]

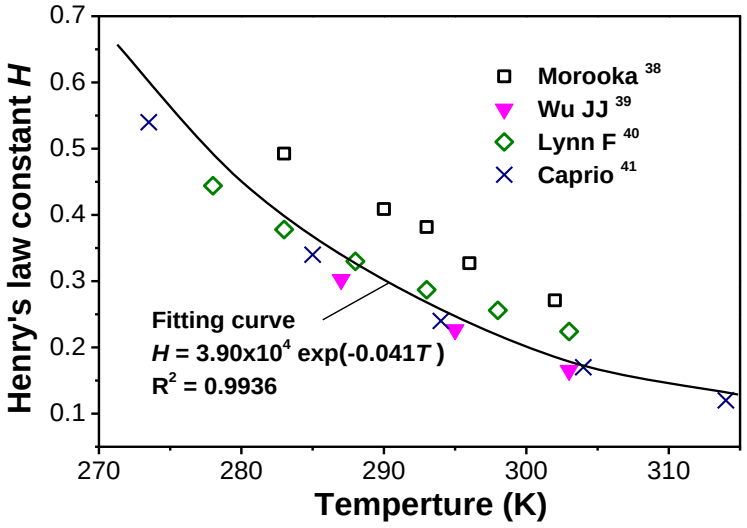

FIGURE 4.3 Solubility of ozone in fresh water (i.e., DI water). The data points are collected from literature and are plotted as dimensionless Henry’s law constant H versus temperature T. The increase of temperature leads to a reduction of Henry’s law constant and consequently a lower ozone solubility in fresh water.

We have collected the reported experimental data of ozone solubility in fresh water as summarized in **FIGURE 4.3**, which plots the dimensionless Henry’s law constant H as a function of the temperature T [111]–[114]. It covers the temperature range from 0 to 45 ^{o}C. In **FIGURE 4.3**, the Henry’s law constant can be fit by $H = 3.90\times10^{4}\exp(-0.041T)$. Therefore, the ozone concentrations in fresh water by pumping the 50-ppm gas phase ozone would be 20.4 μg·L^{-1} and 16.6 μg·L^{-1} at 25 ^{o}C and

30 ^{o}C, respectively.

In sea water, the solubility is even lower. It depends considerably on the concentration of salt. The ozone solubility in the aqueous solutions of NaCl, KCl, Na_2SO_4, $MgSO_4$ and $Ca(NO_3)_2$ were measured at 25 ^{o}C. At each concentration, three to five experiments were carried out; the mean values of the Henry's law constant are listed in **TABLE 4. 2**. The solubility of solutions is generally lower than that of DI water. For instance, the dimensionless Henry's constant is measured to be H = 0.267 in the DI water, but it is only 0.160 for the 0.5-M Na_2SO_4 solution. Nevertheless, it has H = 0.256 for the 0.5-M NaCl solution, only slightly lower than that for the DI water (H = 0.267). This suggests that the solubility of ozone is similar in the fresh water and the 3.5wt% sea water (i.e., 0.6-M NaCl).

TABLE 4. 2 Dimensionless Henry's law constant of ozone in fresh water and salt solutions at 25 ^{o}C. [115]

Concentration	DI water	NaCl	KCl	Na_2SO_4	$MgSO_4$	$Ca(NO_3)_2$
0 M	0.267	–	–	–	–	–
0.5 M	–	0.256	0.255	0.160	0.180	0.203

As discussed above, the dissolved ozone in sea water reacts with the ions and radicals and are then converted to other species. The ozone conversion is strongly affected by the

Cl^- concentration. Here the ozone conversion is defined as the ratio of the amount of converted ozone to the amount of initially dissolved ozone. Based on the study of Sotelo in 1989,[115] an increase of Cl^- concentration leads to an increase of the ozone conversion at a given time. It is read from Sotelo's data curves that at the time of 3 ms, the ozone conversion is 55%, 64%, 83% and > 95% for the NaCl solutions of 0 M (i.e., DI water), 0.05 M, 0.1 M and 0.5 M, respectively. We can see that seawater can quickly absorb almost all ozone as compared to only 55% of the DI water. It implies a better usage of dissolved ozone in the seawater ozonation than in the freshwater ozonation. This is one of the merits of seawater ozonation.

4.4.2 Ozone oxidation in different concentrations of ozone gas

Concentration of ozone strongly affects how fast the oxidation is. The degradation of MB solution using the artificial sea water is measured by varying the ozone concentration as plotted in **FIGURE 4.4 (a)**. It is noted here the ozone concentration refers to the amount of ozone in the pumping gas, not directly the concentration of dissolved ozone in water samples. This is because it is more convenient to measure and is thus used as a control parameter. The amount of dissolved ozone can be calculated based on the above-mentioned relationship $H = H^{cp} \times RT$.

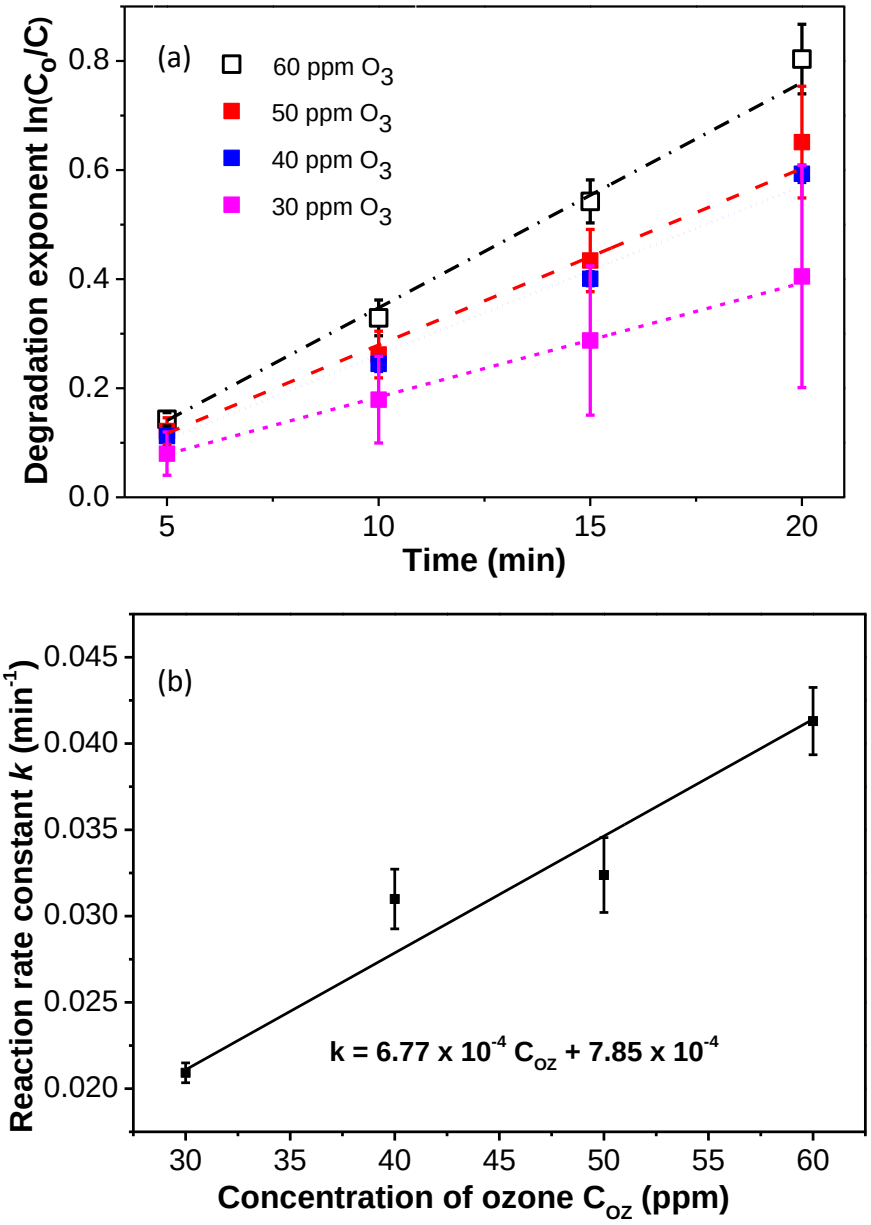

FIGURE 4.4 Measured performance of only the ozonation in sea water. (a) Degradation of methylene blue under different ozone concentrations in the pumping gas. (b) Dependence of the reaction rate constant k on the ozone concentration C_{oz}, which roughly follows a linear relationship $k = 6.77 \times 10^{-4} C_{oz} + 7.85 \times 10^{-4}$ min^{-1}.

In **FIGURE 4.4 (a)**, the vertical axis is the degradation exponent DE as defined by $DE = \ln(C_0/C)$, here ln denotes natural logarithm, C_0 and C are the initial concentration

and the resulted concentration of MB solution, respectively. For the first-order reaction, it should have $C = C_0 \exp(-kt)$, here k is the reaction rate constant and t is the reaction time. For the first-order reaction, it has $DE = kt$. Therefore, the value of DE is linear to t and the slope of the curve DE versus t is just k.

One can see from **FIGURE 4.4 (a)** that an increase of ozone concentration leads to a higher DE. If we look at the error bars (a result of 5 repeated tests), we can see the error range decreases with higher ozone concentration, indicating better repeatability. This might be because ozone is an unstable gas. A higher concentration of ozone could reduce the uncertainty. For safety reason, 0.01 – 8 ppm of dissolved ozone is the maximum limit to human. Here 60 ppm of ozone in gas phase corresponds to 0.026 ppm of dissolved ozone in liquid phase. Therefore, if this study uses maximum 60-ppm ozone in gas, it is far safer than the previous studies that often used more than 5000-ppm ozone for the water treatment. In addition, the use of low ozone concentration helps reduce the cost and is thus favorable for practical applications.

Based on above discussion, the slope of degradation exponent denotes the reaction rate constant. We calculate the slopes of curves in **FIGURE 4.4 (a)** and plot in **FIGURE 4.4 (b)** the relationship with the ozone concentration C_{oz} in the pumping gas. It follows a linear curve $k = 6.77 \times 10^{-4} C_{oz} + 7.85 \times 10^{-5}$ min^{-1}, here C_{oz} is in the unit of ppm.

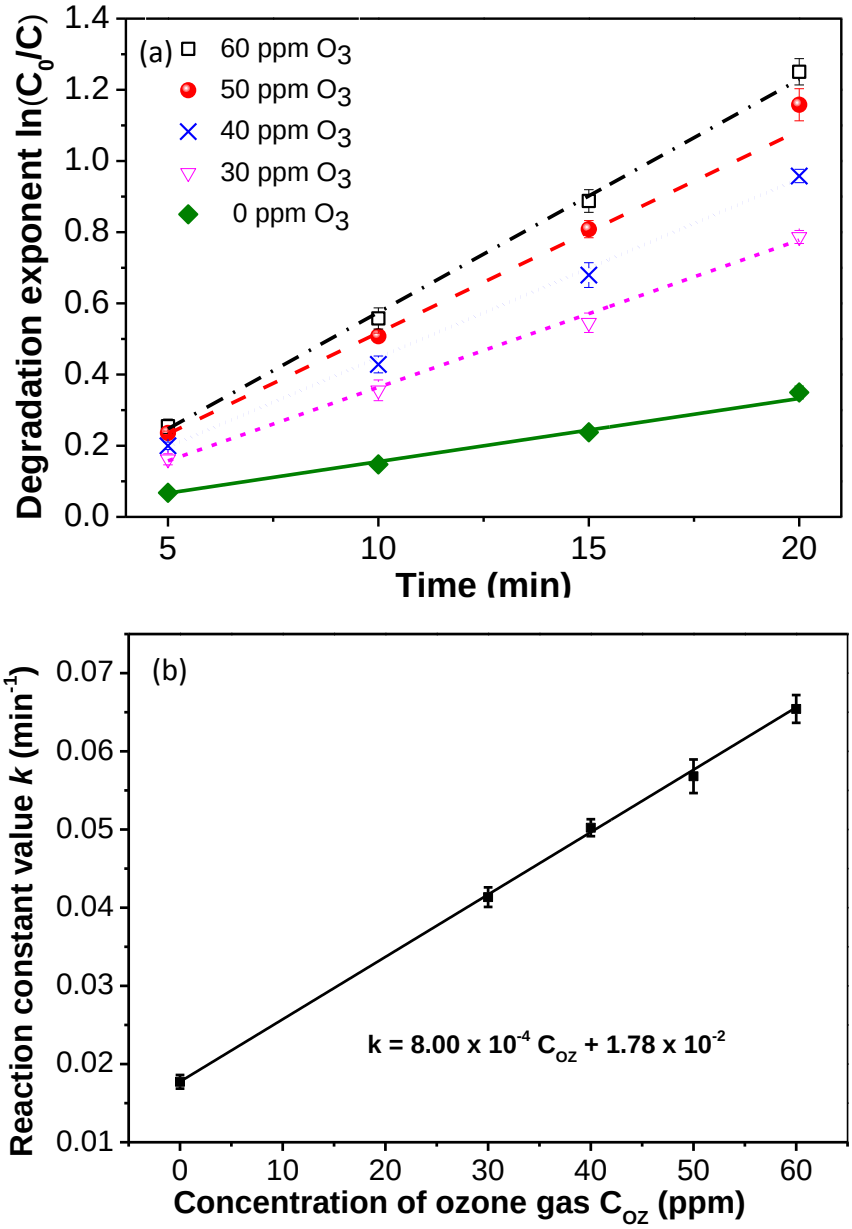

FIGURE 4.5 Measured performance of the photocatalytic ozonation in sea water. (a) Degradation of methylene blue under different ozone concentrations in the pumping gas, in which 0 ppm denotes no ozone and thus the process is only the photocatalysis. (b) Dependence of the reaction rate constant k on the ozone concentration C_{oz}, which closely follows a linear relationship $k = 8.00 \times 10^{-4} C_{oz} + 1.78 \times 10^{-2}$ min^{-1}.

4.4.3 Photocatalytic ozonation: Degradation versus ozone concentration

The efficiency of PCO in sea water have been tested under different concentrations of ozone. The results are plotted in **FIGURE 4.5 (a)**. The photocatalysis without ozone (i.e., 0-ppm ozone) is also plotted as a reference. For a given ozone concentration, the degradation exponent increases almost linearly with *t*. And an increase of ozone concentration results in a higher degradation exponent. Similarly, we plot the slopes of the curves of **FIGURE 4.5 (a)** as a function of the ozone concentration in pumping gas. The result is plotted in **FIGURE 4.5 (b)**, which shows clearly a good linearity. The expression is $k = 8.00 \times 10^{-4} C_{oz} + 1.78 \times 10^{-2}$ min^{-1}. When we compare **FIGURE 4.4 (b)** (for only the ozonation) and **FIGURE 4.5 (b)** (for the PCO), we can see that (i) the data points in **FIGURE 4.5 (b)** have smaller error ranges, showing the PCO in sea water has better stability and repeatability; (ii) **FIGURE 4.5 (b)** has better linearity, showing that the PCO has more controllability; and (iii) The PCO is more effective than the ozonation in the decontamination of seawater. In **FIGURE 4.4 (b)**, it has $k = 6.77 \times 10^{-4} C_{oz} + 7.85 \times 10^{-4}$ min^{-1}, whereas in **FIGURE 4.5 (b)**, it has $k = 8.00 \times 10^{-4} C_{oz} + 1.78 \times 10^{-2}$ min^{-1}. The PCO has the proportional coefficient 8.00×10^{-4} min^{-1}·ppm^{-1}, larger than the value 6.77×10^{-4} min^{-1}·ppm^{-1} of the ozonation. Therefore, the reaction rate constant of PCO

increases more rapidly with the ozone concentration than that of only the ozonation. More importantly, the constant term of *k* factor for the PCO is 1.78×10^{-2} min^{-1}, about 23 times of the constant term 7.85×10^{-4} min^{-1} for the ozonation. These well show that the PCO is better than only the ozonation, which can be regarded as one of the benefits of using the PCO for the decontamination of sea water.

4.4.4 Photocatalytic ozonation: Synergistic effect of photocatalytic ozonation

As stated above, both the photocatalysis and the ozonation play roles in the PCO degradation. However, the PCO efficiency is not simply a summation of the photocatalytic efficiency and the ozonation efficiency. Instead, the PCO efficiency could be higher than the summation of the latter two due to the synergistic effect of photocatalysis and ozonation. To quantify the synergistic effect, we can define a parameter *S* by

$$S = \ln\left(\frac{C_0}{C_{pco}}\right) - \ln\left(\frac{C_0}{C_{pc}}\right) - \ln\left(\frac{C_0}{C_{oz}}\right) = \ln\left(\frac{C_{pc}C_{oz}}{C_0 C_{pco}}\right) \qquad (4.8)$$

where C_{pco}, C_{pc}, C_{oz} are the remaining MB concentrations of the PCO, the photocatalysis and the ozonation, respectively, all at time *t*. This definition is based on the previous expression $C = C_0 \exp(-kt)$, here the terms $\ln(C_0/C_{pco})$, $\ln(C_0/C_{pc})$ and $\ln(C_0/C_{oz})$ represents the reaction rate constants of the PCO, the photocatalysis and the ozonation,

respectively.

Based on the data in **FIGURE 4.4** and **FIGURE 4.5**, the synergistic effect of PCO can be calculated. The results are shown by a 3D plot in **FIGURE 4.6** as the functions of the time and the ozone concentration. For a fixed ozone concentration, the synergistic effect increases with time and then tends to saturate. At a fixed time, the synergistic effect first goes up when the ozone concentration in gas is increased from 30 ppm to 50 ppm; it reaches the maximum at 50 ppm and then goes down at even higher ozone concentration. In this study, 50 ppm is found to be the optimal condition for the synergistic effect of PCO in sea water.

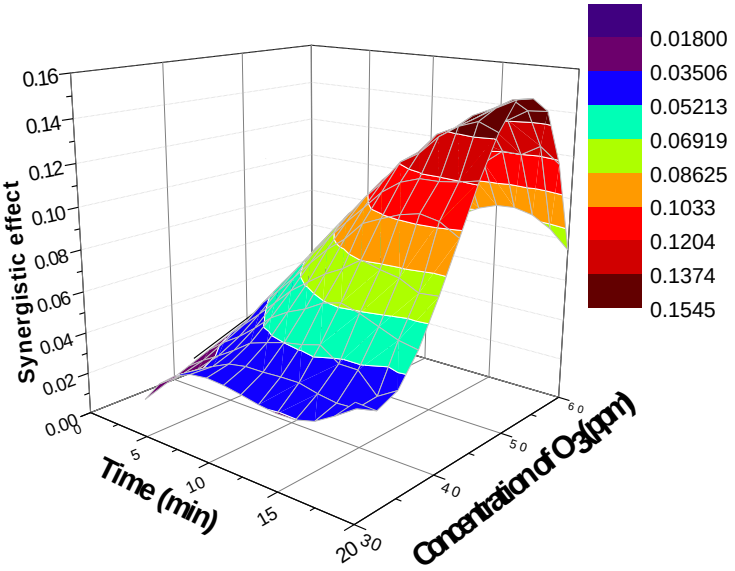

FIGURE 4.6 Synergistic effect of the photocatalytic ozonation in sea water. The synergistic effect is always positive and reaches its maximum when the ozone concentration in the pumping gas is 50 ppm.

4.4.5 Photocatalytic ozonation: Comparison of degradations in fresh water and sea water

Using the optimal concentration of ozone, more thorough degradations of MB in the fresh water (i.e., DI water) and the sea water have been conducted to compare only the photocatalysis, only the ozonation and the PCO effect. The results are plotted and compared in **FIGURE 4.7**. The vertical axis is the degradation, which is defined as $(1-C/C_0)$. In the initial state, the degradation is 0; and if the MB is completed degraded, the degradation becomes 1. Several findings can be observed from **FIGURE 4.7**.

(i) The degradation tends to saturate at high level (degradation > 0.5), this is more obvious when the degradation approaches 1. This is a common phenomenon in oxidative degradation.

(ii) The fresh water has always higher degradation than the sea water, regardless of photocatalysis, ozonation or PCO. This matches the above prediction (in the mechanism part) that the sea water has weaker oxidation power since the Cl^- ions convert highly oxidative radicals like $^*OH$ and O_3^- into relatively weak radicals like OCl^* and $^*ClO_3$.

(iii) The fresh water has smaller error ranges than the sea water. Again, this is because the salt ions disturb the oxidation process and causes uncertainty.

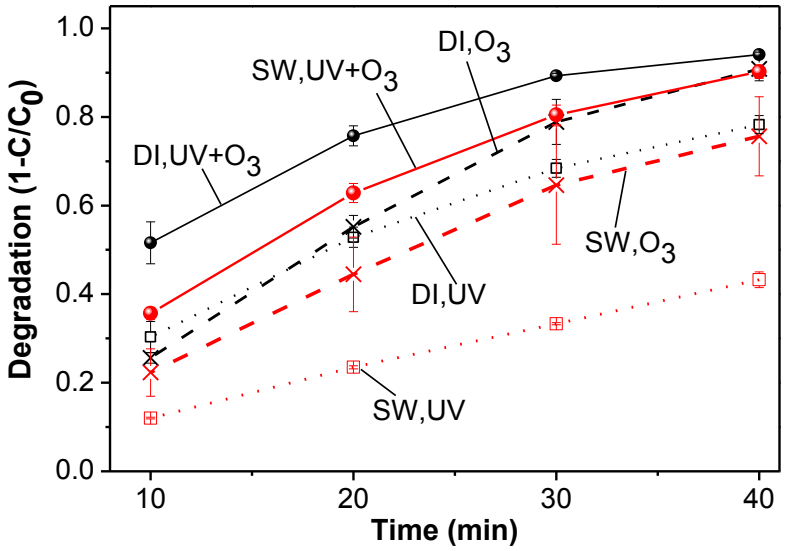

FIGURE 4.7 Comparison of the degradations of methylene blue in fresh water (i.e., DI water) and sea water by the photocatalysis, the ozonation and the photocatalytic ozonation. Under the same condition, the fresh water always shows higher degradation efficiency than the sea water. Labels: SW for sea water, UV for photocatalysis, O_3 for ozonation, and UV+O_3 for photocatalytic ozonation.

4.4.6 Photocatalytic ozonation: Comparison of synergistic effects in fresh water and sea water

As discussed above, the fresh water has always higher degradation than the sea water. Consequently, the fresh water may have smaller synergistic effect than the sea water. **FIGURE 4.8** compares the synergistic effects of the PCO in fresh water and sea water under 50 ppm ozone. In sea water, the synergistic effect increases slightly with the lapse of time. Oppositely, the synergistic effect of fresh water becomes negatively and further drops quickly with time. The reason might be that 50-ppm ozone is not the optimal condition for the PCO in fresh water. Instead, it is too high to make the direction oxidation reaction of ozone dominant, and thus the high ozone concentration would reduce the

synergistic effect to negative.

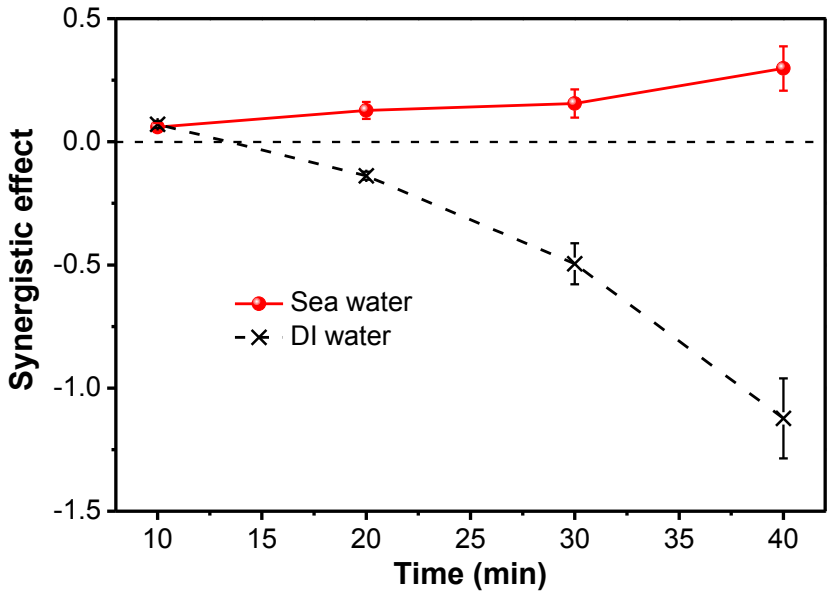

FIGURE 4.8 Comparison of the synergistic effects in fresh water (i.e., DI water) and sea water when the pumping gas has the ozone concentration of 50 ppm, which is optimal for the photocatalytic ozonation of sea water.

4.4.7 Photocatalytic ozonation: Influence of salt concentration on degradation efficiency

To examine the influence of salinity, the PCO experiments are conducted using the artificial sea water with different salt concentrations. The results are plotted in **FIGURE 4.9**. It shows clearly that a lower salinity leads to a higher degradation efficiency, but the difference is not that large. At the sampling times of 20 s, 30 s and 40 s, the highest degradation occurs at the 25% concentration (corresponding to 0.875 wt%), not at 0% (i.e., fresh water). As stated above, the salt ions increase the conversion of dissolved ozone, but they convert the highly-oxidative ions (e.g., *OH) into relatively weak ions

(e.g., Cl^*, OCl^*) and thus lower the oxidizing power. 25% concentration of sea water may make a good trade-off between these two factors and thus results in the optimal degradation.

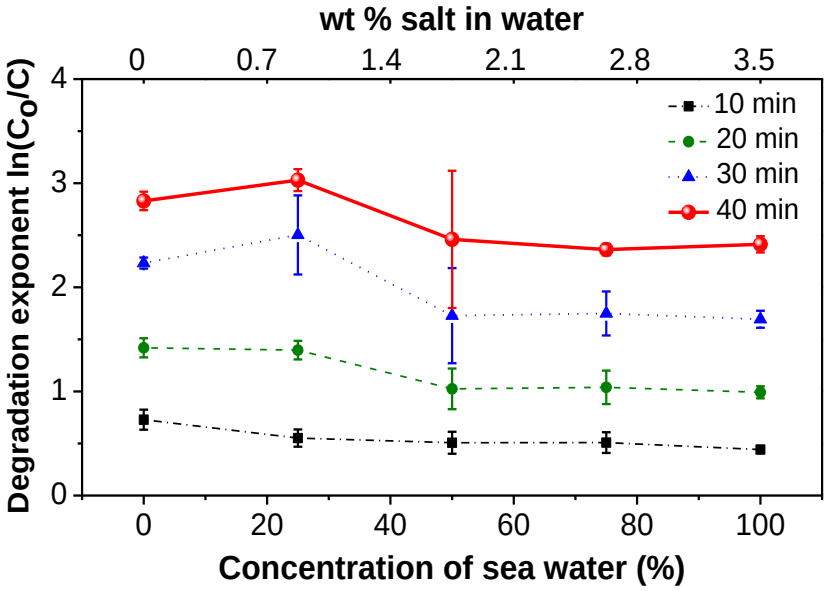

FIGURE 4.9 Degradation performance in sea water with different salt concentrations. The upper *x* axis is the weight percentage of salt in water, whereas the lower *x* axis is the relative concentration to the standard 3.5wt% sea water.

TABLE 4. 3 Functional effects in different treatments and their influences on the synergistic effect.

	Photolysis effect	Photocatalytic effect	Ozonation effect
Photocatalysis process	Yes	Yes	–
Ozone process	–	–	Yes
PCO process	Yes	Yes	Yes
Synergistic effect	**Removed**	**Included**	**Included**

4.4.8 Photocatalytic ozonation: Influence of UV photolytic effect on synergistic effect

UV photolysis of MB dyes may affect the photocatalysis treatment and the PCO treatment. **TABLE 4. 3** lists the major effects in each treatment. Fortunately, the definition of synergistic effect in **Equation 4.8** uses the PCO to deduct the photocatalysis, which makes sure that the contribution of UV photolytic effect is already removed.

4.5 Summary

Polluted sea water is a common problem in coastal cities, but its decontamination remains a big challenge due to the existence of salt ions, which may invalidate many prevailing treatment methods originally developed for waste fresh water. This work presents the first attempt to decontaminate the polluted sea water by synergizing two separate processes: photocatalysis and ozonation. For low cost and human safety, the ozone concentration is kept to be < 60 ppm in the pumping gas (0.026 ppm in solution). Mechanism studies and experimental comparisons show that the photocatalysis, the ozonation and the photocatalytic ozonation (PCO) all have lower efficiency in sea water than in fresh water, and the PCO is always more efficient than only the photocatalysis or only the ozonation. More specifically, the PCO has a reaction rate constant about 23 times higher than only the ozonation. In addition, the sea water shows a positive synergistic effect of photocatalysis and ozonation and reaches the maximum when the pumping gas has an ozone concentration of 50 ppm in gas. In contrast, the fresh water shows a negative synergistic effect. This work may pave the way to practical applications of sea water decontamination with high efficiency and low cost by using both UV and ozone. In the next chapter, the combined use of both UV and ozone will be applied to another important application – bacteria disinfection.

CHAPTER 5. UV-OZONATION FOR BACTERIA DISINFECTION

The previous chapter combines the UV photocatalysis and the ozonation for seawater treatment. In this work, we will combine the UV irradiation and the ozonation for another important application – bacteria disinfection. Many sterilization techniques have already been developed but they are subject to some limitations. For instance, chlorine disinfection is most widely used, but it produces harmful by-products during the disinfection process; ozone treatment may produce mutations such as macromolecule organic substances that threat human health; and UV disinfection is fast and produces no by-products, but the inactivated bacteria may be reactivated in sunlight or dark environment and proliferate afterwards due to the light resurrection effect.

To overcome these problems, this study utilizes both the UV light and the ozone to disinfect the bacteria in fresh water. The UV light deactivates the bacteria and the dissolved ozone suppresses the photo-resurrection. The combined use of both processes ensures the disinfection of bacteria with high efficiency, low cost and no harmful by-products.

5.1 Preparation and equipment

The artificial waste water is diluted from nutrient broth by normal saline to 10^6 cfu/ml. In the dilution, some nutrient broth is added into the solution to simulate the nutrition in the waste water after the treatment. After the treatment, 0.1 mL of the solution is put into an agar plate for cultivation at 37℃ for24 hour.

In this study, a 25W UV-C lamp is used as the light source. The lamp emits UV light at 254 nm. It is put into a water bath for temperature control. The sample solution would pass through a quartz spiral tube in **FIGURE 5.1**. The distance between the tube and the lamp is less than 1 cm to ensure most of the light energy falls on the solution. The exposure time (or equivalently, residence time, or reaction time) is controlled by the flow rate of the pump, which feeds the sample solution into the tube. An ozone generator is used in the ozone treatment part. The generator with the power of 35 W generates ozone by high voltage discharge. And the ozone is then pumped into the solution directly. Before the disinfection experiment, the relationship between the pumping time and the concentration of ozone in the water should be tested. Since the ambient air is needed to generate the ozone, the ozone concentration in air is affected by the relative humidity. Therefore, the relationship between the concentration of dissolved ozone and the pumping

time varies day to day and should be calibrated using iodometry every time before the disinfection experiment.

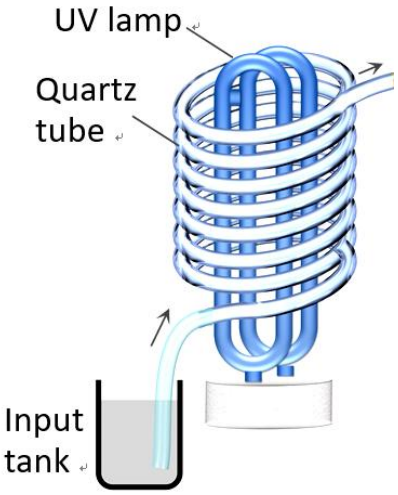

FIGURE 5.1 Experiment set up for bacteria disinfection by UV-ozonation.

5.2 Experiment process

At the beginning, the artificial waste water with 10^6 CFU/mL is used to prepare 3 samples onto agar plates to verify the concentration of the bacteria. In the disinfection experiments the solution is pumped into the quartz spiral tube, and the exposure time under UV-C is controlled to be 0.5s, 1s, 1.5s and 2s by adjusting the flow rate of the pump. After the treatment, 3 samples are put onto agar plates to measure the bacteria concentration and to determine the efficiency of UV treatment. Next, ozone is pumped in. Until the concentration of dissolved ozone reaches 0.5 ppm in water. The pumping time needed is usually shorter than 1 min. After the ozone treatment, 3 samples are also taken to cultivate

in the agar plates to determine the efficiency of UV-ozone method. For control experiment, some artificial waste water is pumped with only ozone (without the UV treatment) to determine the efficiency of single ozone treatment.

In the above experiments, all samples are put into the sterilized bottles and will be placed at light environment and dark environment for 24 hours, separately. This is to check the bacteria proliferation and the photo-resurrection.

TABLE 5. 1 Diameters of the cultivated colonies of different treated solutions.

		Right after UV disinfection	After UV disinfection & 24 hours in dark	After UV disinfection & 24 hours in light	After ozone treatment
Control solution		3.07 mm	2.99 mm	3.02 mm	3.06 mm
Exposure time of UV	0.5s	0.5 mm	0.55 mm	0.37 mm	The diameter of the colony after ozone treatment: 3.14 mm
	1s	1.33 mm	0.91 mm	1.65 mm	
	1.5s	1.72 mm	0.93 mm	1.76 mm	
	2s	2.08 mm	2.73 mm	1.86 mm	

5.3 Results and discussion

This study consists of two separated parts: qualitive and quantitative.

5.3.1 Qualitative study

The quality of bacteria can be represented by the size of the colony. Larger size indicates a better quality. And the size of the bacteria has been compared and showed in **TABLE 5. 1** and **FIGURE 5.2**:

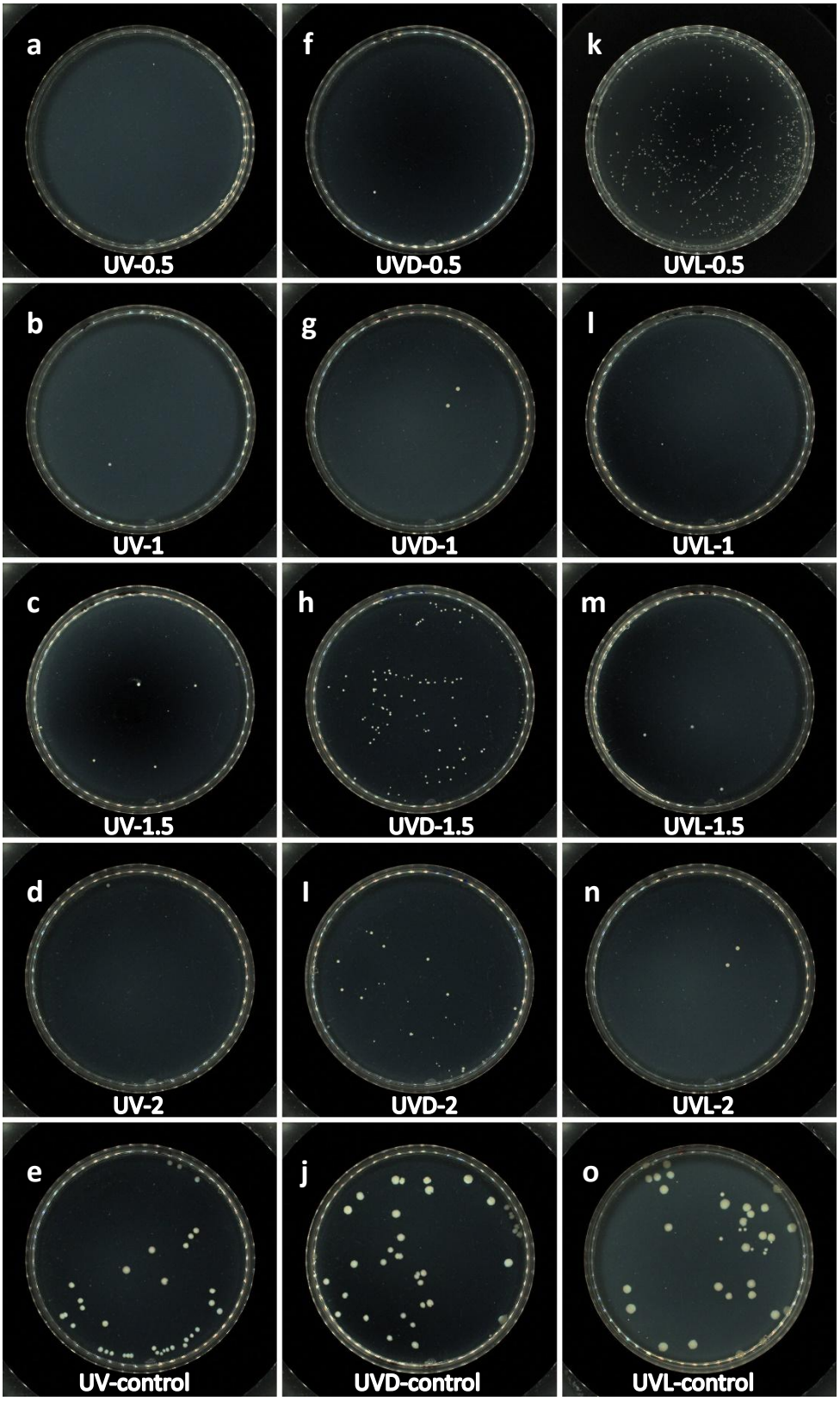

FIGURE 5.2 The photos of the colony on the agar plate for different samples.

In **FIGURE 5.2**, (a-d) show the bacteria colonies right after the UV exposure for 0.5 s, 1 s, 1.5 s and 2 s, respectively (the relative figures are labeled as UV-0.5; UV-1; UV-1.5; UV-2); (e) represents the colony of the control sample (i.e., diluted solution, no UV exposure) (the relative figure is labeled as UV-control); (f)-(i) show the colonies whose solution sources are treated by UV exposure for 0.5 s, 1 s, 1.5 s and 2 s and then stored in dark for 24(the relative figures are labeled as UVD-0.5; UVD-1; UVD-1.5; UVD-2); (j) is the colony of another control sample which is diluted and placed in dark for 24 (the relative figure is labeled as UVD-control); (k)-(n) are the colonies whose source solution are exposed to UV for 0.5 s, 1 s, 1.5 s and 2 s and then are placed in light for 24 (the relative figures are labeled as UVL-0.5; UVL-1; UVL-1.5; UVL-2); and (o) is the colony of another control sample which is diluted and placed in light for 24 (the relative figure is labeled as UVL-control).

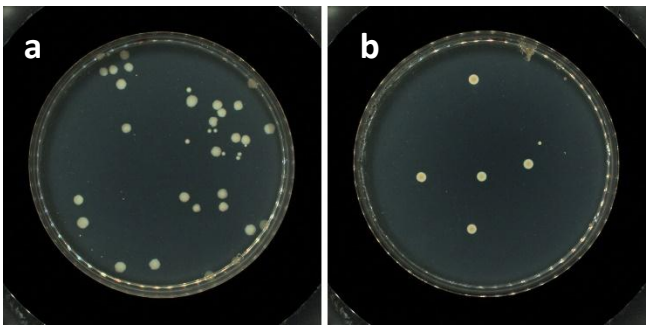

FIGURE 5.3 The photos of the colony on the agar plate for different samples by ozone treatment.

In **FIGURE 5.3**, (a) represents the colony of the control sample after ozone treatment; (b) show the colonies whose solution sources are treated by ozone treatment (i.e. dissolved ozone of 0.5ppm in water)

One can see from **TABLE 5. 1** and **FIGURE 5.2** that the colony size of the UV exposed solution is reduced. This is because the UV exposure dimerizes the adjacent thymine bases of the nucleic acid strands and prevents accurate transcription of the DNA strand cannot occur, therefore the bacteria cell cannot divide and proliferate. As a result, the bacteria are first weakened and then killed. On the other hand, the sample treated by ozone shows the similar colony size as compared to the reference colony. The reason is that the ozone changes proteins and the unsaturated bonds of fatty acids in the cell membrane. Therefore, the bacteria are directly killed, without the weakened stage.

The solution after both the UV exposure and the ozone treatment does not show any bacteria colonies, inferring the complete disinfection. This proves that the UV and ozone method is very efficient.

5.3.2 Quantitative study

For the quantitative analysis, here we define the disinfecting rate *Dr* as:

$$D_r = \log(\frac{N}{N_o}) \qquad (5.1)$$

where N is the number concentration of bacteria in the treated solution (unit: CFU/mL) and N_o is that in the solution before the treatment.

FIGURE 5.3 plots the disinfecting rate as a function of the UV exposure time for 3 different solutions, including the solution right after the UV disinfection, the solution after UV exposure and the placed in dark for 24 hours and the solution after UV exposure and placed in light for 24 hours. If the value of $\log(N/N_o)$ is smaller, the efficiency of disinfection is better. The results of the solution just finished disinfection shows the disinfecting rate is from -4.98 to -5.83. And the rate goes down when the exposure time is longer. The results prove that single UV disinfection can be used to disinfect the waste water of 10^5 CFU/mL bacteria.

It is a common problem that the UV deactivated bacteria may be reactivated under light irradiation. Our experiment matches the prediction. When the water sample disinfected is placed at rest in light for 24 hours, and found out more bacteria inside the solution. And the disinfecting rate deteriorates to between -4.4 to -5.03. And the relation between the disinfecting rate is similar to that of the solution right after the UV disinfection. On the other hands, additional samples are placed at rest in a dark place for 24h. The results show nearly the same disinfecting rate with the solution of just finishing disinfection. This clearly proves the light resurrection phenomenon in the UV disinfection.

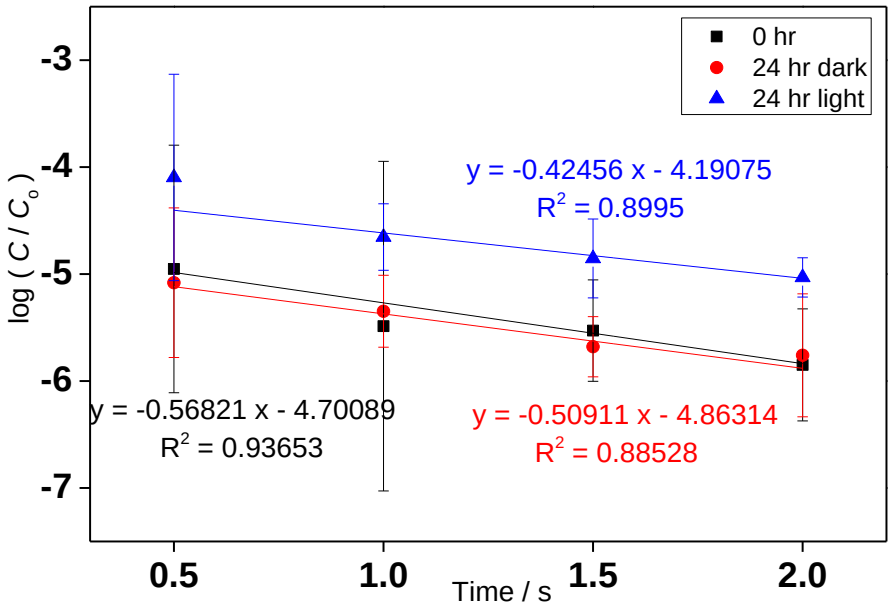

FIGURE 5.4 Disinfecting rates of the samples right after UV disinfection, placed for 24 hours in dark and in light, respectively.

In some countries, waste water treatment works usually build a long sewer to avoid the problem of light resurrection. So as to meet the regulation criteria. At the end of the sewer is the test point by government. In this way, the test data look good for the quality control of waste water effluent, but the bacteria concentration would go up after the effluent is disposed into surface water and is subject to sunlight. My study is to solve this problem completely by a dual method that, combines both the UV irradiation and the ozone disinfection.

TABLE 5. 2 Disinfecting rate of the ozone treatment

	The sample of finishing ozone disinfection	The sample placed at rest for 24 hours after ozone disinfection
Disinfecting rate	-1.678	-1.53

The disinfecting rate of single ozone disinfection is listed in **TABLE 5. 2**. It is -1.678 right after the ozone treatment and becomes -1.53 after the treated sample is placed in dark for 24h. In contrast, if the samples are treated by the dual method, no bacteria can be found after the cultivation. This shows the dual method has the best performance in my study.

The above observations result from the different disinfecting mechanisms of the UV disinfection and the ozone disinfection. The former weakens and kills the bacteria by dimerizing adjacent thymine bases of the nucleic acid strands, and thus suppresses the accurate transcription of that DNA strand and the division of bacteria cell. In contrast, the latter changes the proteins and the unsaturated bonds of fatty acids in the cell membrane. In other words, the UV light kills the bacteria from inside while the ozone destroys the bacteria from outside. The combination of both enables to disinfect the bacteria more efficiently.

5.4 Summary

This chapter applies both UV light and ozone to the disinfection of residual bacteria in waste water. Experiment studies find that: (i) both UV light and ozone can disinfect efficiently; (ii) light resurrection is severe for the UV disinfection but not serious for the ozone disinfection; (iii) the successive use of the UV and ozone can completely kill the bacteria. With these, we can see that the combination of UV and ozone disinfections has great potential to the disinfection of waste water effluent with light efficiency and low cost.

CHAPTER 6. CONCLUSIONS AND FUTURE WORK

6.1 Conclusion

This research study has covered three parts with the view of real applications, including the solar reactors for water purification, the photocatalytic ozonation for seawater decontamination and the combined method of UV and ozone for water disinfection.

The study of real application has been finished by developing a new design of reactor, which is large-size, closed-chamber, light weight and nonbrittle. Experimental tests show a degradation of 30%of MB when the reaction is operation for 2 hours in outdoor sunlight by that reactor. Although the efficiency is not high, it is already 23.6 times of the photolysis, and the use of sunlight is abundant, environment friendly.

The photocatalytic ozonation for seawater decontamination has been finished by finding out the best concentration of ozone in the process and by using the synergistic effect of the photocatalysis and the ozonation. For low cost and human safety, the ozone concentration is kept to be < 60 ppm in the pumping gas (0.026 ppm in solution). More specifically, the PCO has a reaction rate constant about 23 times higher than only the ozonation.

The combined method of UV and ozone for water disinfection has been accomplished by the successive use of the UV disinfection and the ozonation, which is experimentally observed to enable full disinfection of bacteria in the efficiency of waste water treatments work. and avoid the photo-resurrection.

With the research study of this M. Phil. study, I am able to deal with the major problems of waste water treatment: the polluted fresh water can be decontamination by

the solar reactor in chapter 3, the polluted sea water can be decomposed by the photocatalytic ozonation method in chapter 4, and the residual bacteria in the waste water can be disinfected by the UV-ozone method developed in chapter 5. Therefore, this M. Phil. study us highly potential for practical applications of waste water treatment.

6.2 Future work

In the future, more experimental and design efforts will be devoted to improving the efficiency of waste water treatment, as succinctly depicted as follows:

(1) Regarding the large-size reactor, the thickness of the water layer is the key factor of the efficiency of the reactor. The new design can try to develop the water layer to < 100 μm.

(2) Regarding the photocatalytic ozonation of seawater, although the combine method can increase the degradation efficiency by over 20 times, ozone is still not very stable in water. Other chemicals which is highly oxidative can be used to replace ozone.

(3) Regarding the combined method of UV and ozone for water disinfection, the cost for the treatment is relatively high as compared to the original treatment method. The next research direction can aim to reduce the bacteria in the water before entering waste water treatment process.

REFERENCES

[1] Y. Tang, C. Hu, and Y. Wang, "Recent Advances inMechanisms and Kinetics of TiO_2 Photocatalysis," *Prog. Chem.*, vol. 14, no. 3, pp. 192–199, 2002.

[2] X. Yu, J.J. Cheng, and Y. Du, "TiO_2 Photocatalytic Material," *Chem. World*, vol. 11, pp. 567–570, 2000.

[3] R. Goslich, R. Dillert, and D. Bahnemann, "Solar water treatment: Principles and reactors," *Water Sci. Technol.*, vol. 35, no. 4, pp. 137–148, 1997.

[4] M. I. Litter, "Heterogeneous photocatalysis: Transition metal ions in photocatalytic systems," *Appl. Catal. B Environ.*, vol. 23, no. 2, pp. 89–114, 1999.

[5] C. Minero, "Large solar plant photocatalytic water decontamination: Effect of operational parameters," *Sol. Energy*, vol. 56, no. 5, pp. 421–428, 1996.

[6] M. R. Hoffmann, M. Scot T., W. Choi, and D. W. Bahnemann, "Environmental Applications of Semiconductor Photocatalysis," *Chem. Revie*, vol. 95, no. 1, pp. 69–96, 1995.

[7] S. Yan, W. Luo, Z. Li, and Z. Zou, "Progress in Research of Novel Photcatalytic materials," *Mater. China*, vol. 29, no. 1, p. 1–9,53, 2010.

[8] A. Fujishima and K. Honda, "Electrochemical Photolysis of water at a semiconductor electrode" *Fujishm A, Hond K.*, vol. 238, pp. 37–38, 1972.

[9] J. Jing and L. Wang, "Photoctalytic Oxidation of Environment Organic Pollution Using TiO_2 as the Catalyst," *Pollut. Control Technol.*, vol. 12, no. 2, 1999.

[10] Z. Wang *et al.* , "Preparation and Photocatalytic Activity of TiO_2/Graphene Composites," *J. Mater. Sci. Eng.*, vol. 29, no. 2, p. 267–271,232, 2011.

[11] Y. Hu, H. Liu, and X. Guo, "Research progress on Nitrogen doped Titania

Photocatalyst," *J. chinese Ceram. Soc.*, vol. 38, no. 3, pp. 535–541, 2010.

[12] W.Z. Wang, M. Shang, W.-Z. Yin, J. Ren, and L. Zhou, "Recent Progress on the Bismuth Containing Complex Oxide Photocatalysts," *J. Inorg. Mater.*, vol. 27, no. 1, pp. 11–18, 2012.

[13] X. Liu and J. Li, "Development of photocatalysis material for bismuth titanate compounds," *China Ceram.*, vol. 45, no. 10, pp. 10–11, 2009.

[14] A. Kudo and S. Hijii, "H_2 or O_2 evolution from aqueous solutions on lay-ered oxide photocatalysts consisting of Bi^{3+} with 6_s^2 configuration and d_0 transition metal ions.," *Chem. Lett.*, vol. 28, no. 10, p. 1103−1104, 1999.

[15] J.W. Tang, Z.G. Zhou, and J.H. Ye, "Photocatalytic decomposition of organic contaminants by Bi_2WO_6 under visible light irradation," *Catal. Lett.*, vol. 92, no. 1-2, pp. 53–56, 2004.

[16] C. Zhang and F.Y. Zhu, "Synthesis of square Bi_2WO_6 nanoplates as high-activity visible-light-driven photocatalysts.," *Chem. Mater.*, vol. 17, no. 13, p. 3537−3545, 2005.

[17] E. Li, L. Chen, Q. Zhang, W. Li, and S. Yin, "Bismuth Containing Semiconductor Photocatalysts," *Prog. Chem.*, vol. 22, no. 12, pp. 2282–2289, 2010.

[18] A. Kudo, K. Omori, and H. Kato, "A novel aqueous process for preparation of crystal form-controlled and highly crystalline $BiVO_4$ powder from layered vanadates at room temperature and its photocatalytic and photophysical properties," *J. Am. Chem. Soc.*, vol. 121, no. 49, p. 11459−11467, 1999.

[19] S. Tokunaga, H. Kato, and A. Kudo, "Selective preparation of monoclinic and tetragonal $BiVO_4$ with scheelite structure and their photocatalytic properties,"

Chem. Mater., vol. 13, no. 12, p. 4624−4628, 2001.

[20] T. Zhai, X. Fang, L. Li, Y. Bando, and D. Golberg, "One-dimensional Cd-S nanostructure: synthesis, properties, and application," *Nanoscale*, vol. 2, no. 2, pp. 167–187, 2010.

[21] A. Kudo, K. Ueda, and H. Kato, "Photocatalytic O_2 evolution under visible light irradiation on $BiVO_4$ in aqueous $AgNO_3$ solution," *Catal. Lett.*, vol. 53, no. 3, p. 229−230, 1998.

[22] R. Zhao, X. Li, and Z. Xu, "Controlled Synthesis and Photocatalytic Activity of CdS with Different Morphologics in Ionic Liquids," *Mater. Rev. B Res.*, vol. 28, no. 9, pp. 18–22, 2014.

[23] G. Guo, S. Ding, and J. Li, "Progress on Visible-light-respond Photocatalytic materials," *Hebei Chem. Eng. Ind.*, no. 5, pp. 6–9, 2004.

[24] X. Wang, X. Zhang, and C. Fan, "Resesarch and development of BiOCL-based photocatalytic materials," *Chem. Ind. Eng. Prog.*, vol. 33, no. 1, p. 124–132,149, 2014.

[25] C. Xu, Y. Han, and M. Chi, "Cu_2O-Based Photocatalysis," *Prog. Chem.*, vol. 22, no. 12, pp. 2290–2297, 2010.

[26] C. Zhang, C. Zheng, and G. Zhang, "Preparation of TiO_2/ZnO coupled-semiconductor photocatalyst by microwae irradiation method," *Chenical Eng.*, no. 22, pp. 20–23, 2007.

[27] K. Krishnamoorthy, R. Mohan, and S.J. Kim, "Graphene Oxide as a photocatalytic material," *Appl. Phys. Lett.*, vol. 98, no. 24, p. 244101-114312, 2011.

[28] S. Min and G. Lu, "Preparation of CDS/Grapgene Composites and Photocatalytic

Hydrogen Generation from water under Visible Light Irradiation," *WuLi Huaxue Xuebao*, vol. 27, no. 9, pp. 2178–2184, 2011.

[29] X. Yang and Y. XU, "Study on partical photocatalysis reactor of TiO_2," *Appl. Chem. Ind.*, vol. 38, no. 1, p. 124–127,141, 2009.

[30] Z. Shi, S. Zhang, and Z. LIN, "Progress of studies on solar energy photocatalytic reactor," *Chem. Ind. Eng. Prog.*, vol. 26, no. 9, pp. 1223–1227, 2007.

[31] Y. Ao, X. Shen, C. Yuan, and D. Fu, "The Development of Inorganic Adsorbent Mounted TiO_2 in Organic Contamination Treatment," *Saf. Environ. Eng.*, vol. 13, no. 1, pp. 37–40, 2006.

[32] Y. Zhang, "Research Progress on Suspension and Fluidized Bed Nano TiO_2 Photocatalytic Reacger," *Environ. Prot. Sci.*, vol. 35, no. 6, pp. 7–9, 2009.

[33] J. Fu, M. Ji, Z. Wang, L. Jin, and D. An, "A new submerged photocatalysis reactor(SMPR) for fulvic acid removle using a nano-sturcture photocatalyst," *J. Hazard. Mater.*, pp. 238–242, 2006.

[34] G. Jia, Y. Zhang, X. Zhang, and F. Chu, "Dynamis Expimental Research on Photocatalytic Degradation of Phenol in Waste Water Using TiO_2/ACF," *J. NanJing Norm. Univ. Technol. Ed.*, vol. 9, no. 2, pp. 52–55, 2009.

[35] X. Yin, C. Sun, F. Xin, F. Zhang, S. Wang, and G. Zhang, "Desgin and simulation of novel rotating cylinder photocatalytic reactor," *J. Chem. Ind. Eng.*, vol. 59, no. 1, pp. 77–83, 2008.

[36] C. Passalia, O.M. Alfano, and R.J. Brandi, "A methodology for modeling photocatalytic reactors for indoor pollution control using previously estimated kinetic parameters," *J. Hazard. Mater.*, pp. 357–365, 2012.

[37] Q. Geng, Q. Guo, C. Cao, and L. WANG, "Review of heterogenous photocatalytic reactor," *Chenical Ind. Eng. Prog.*, vol. 27, no. 1, pp. 68–73, 2008.

[38] G. Cao, R. Luo, and B. Ren, "Development of the heterogeneous photoctalytic reactor in wastewater treatment," *Tech. Equip. Envirment Pollut. Control*, vol. 4, no. 1, pp. 73–76, 2003.

[39] M.M. Ballari, O.M. Alfano, and A.E. Cassano, "Mass transfer limitation in slurry photocatalytic reactor: Experiment validation," *Chem. Eng. Sci.*, pp. 4931–4942, 2010.

[40] S. Lin and T. Li, "Effciency evalation of solar photocatalytic reactor with immobilized catalyst," *J. Chem. Ind. Eng.*, vol. 59, no. 1, pp. 90–95, 2008.

[41] G.E. Romanos *et al.* , "Double-silde active TiO2-modified nanofilration membranes in continuous flow photocatalytis reactord for effective water purification," *J. Hazard. Mater.*, pp. 304–316, 2012.

[42] Y. Wang, Y. Fu, and H. Tang, "Solar photocatalytic degradation of methyl Organe with a non concen-trating flat-plate photoreactor," *Acta Sci. Circumstantiae*, vol. 19, no. 2, pp. 142–146, 1999.

[43] H. Li, Z. Hao, L. Zhang, S. Liu, and F. Zhang, "Influence of Stursture of Labyrinth Photocatalytic reactor on degradation performance of Methyl Organe," *J. Taiyuan Univ. teachnology*, vol. 39, no. 3, pp. 226–229, 2008.

[44] X. Hao, S. Luo, Z. Zhang, C. Fan, S. Liu, and Y. Sun, "Photocatalytic Degradation Performance of Phenol in Wastewater Using a Novel Labyrinth Bubble Photoreactor," *J. Chem. Eng. China Univ.*, vol. 21, no. 6, pp. 1056–1059, 2007.

[45] Y. Zhang, Y. Yu, and Q. Liu, "Progress in multiphases photocatalytic degradation

of dye-containing wastewater," *Ind. Water Treat.*, vol. 21, no. 12, pp. 1–4, 2001.

[46] X. Yan, X. Li, K. Song, M. Huo, and J. Wang, "Research progress in Fixed photocatalyst TiO_2 and Photo Reactor," *Chem. Ind. Eng. Prog.*, no. 2, p. 12–14,18, 2002.

[47] G.P. Li, J. Khor, and A. Brucato, "Modeling of an Annular Photocatalytic Reactor for water Purification Oxidation of Pesticides," *Environ. Sci. Technol.*, vol. 38, pp. 3737–3745, 2004.

[48] P. Cui, Y. Fan, N. Xu, and J. Shi, "Design and Application of Fludized bed photocatalytic reactor," *J. Chem. Ind. Eng.*, vol. 52, no. 3, pp. 195–196, 2001.

[49] D. Fu, "Research on the Loading Method of Nanometer Photocatalysis Material," *Jiangxi Chem. Ind.*, no. 4, pp. 50–51, 2014.

[50] X. Wang, X. Li, F. Liu, X. Wang, and C. Sun, "The effect Research and Surface Coating Technology Preparation of Photocatalysis Material," *J. Shandong Jiaotong Univ.*, vol. 13, no. 4, pp. 57–59, 2005.

[51] Z. Dai, A. Chen, H. Gu, Z. Zhu, and M. Gu, "Model and experiemtn verification of radiation energy distribution in novel packed-bed photocatalytic reactor," *J. Chem. Ind. Eng.*, vol. 53, no. 8, pp. 775–779, 2002.

[52] D. Bahnemann, "Photocatalytic water treatment: Solar energy applications," *Sol. Energy*, vol. 77, no. 5, pp. 445–459, 2004.

[53] J. Herrmann, "Heterogeneous photocatalysis : state of the art and present applications," *Top. Catal.*, vol. 34, pp. 49–65, 2005.

[54] T.M. Elmorsi, Y.M. Riyad, Z.H. Mohamed, H.M.H. Abd, and E. Bary, "Decolorization of Mordant red 73 azo dye in water using H_2O_2 / UV and photo-

Fenton treatment," *J. Hazard. Mater. J.*, vol. 174, pp. 352–358, 2010.

[55] H. Ghodbane and O. Hamdaoui, "Decolorization of antraquinonic dye , C . I . Acid Blue 25 , in aqueous solution by direct UV irradiation , UV / H_2O_2 and UV/Fe (II) processes," *Chem. Eng. J.*, vol. 160, no. 1, pp. 226–231, 2010.

[56] R. Yuan, S.N. Ramjaun, Z. Wang, and J. Liu, "Photocatalytic degradation and chlorination of azo dye in saline wastewater : Kinetics and AOX formation," *Chem. Eng. J.*, vol. 192, pp. 171–178, 2012.

[57] L. Hu, P.M. Flanders, P.L. Miller, and T.J. Strathmann, "Oxidation of sulfamethoxazole and related antimicrobial agents by TiO_2 photocatalysis," *water reaserch*, vol. 41, pp. 2612–2626, 2007.

[58] J. Nath and B. Corresponding, "Degradation of Antibiotics (Trimethoprim and Sulphamethoxazole) Pollutants Using UV and TiO_2 in Aqueous Medium," *Mod. Appl. Sci.*, vol. 3, no. 2, pp. 3–13, 2009.

[59] A.G. Trovó, R.F.P. Nogueira, A. Agüera, C. Sirtori, and A. R. Fernández-alba, "Chemosphere Photodegradation of sulfamethoxazole in various aqueous media : Persistence , toxicity and photoproducts assessment," *Chemosphere*, vol. 77, no. 10, pp. 1292–1298, 2009.

[60] R.F.P. Nogueira, A. Agu, and A.G. Trovo, "Degradation of sulfamethoxazole in water by solar photo-Fenton . Chemical and toxicological evaluation," *water Res.*, vol. 43, pp. 3922–3931, 2009.

[61] C.C. Yang, C.L. Huang, T.C. Cheng, and H.T. Lai, "Inhibitory effect of salinity on the photocatalytic degradation of three sulfonamide antibiotics," *Int. Biodeterior. Biodegrad.*, vol. 102, pp. 116–125, 2015.

[62] D. Wang, "The Application of TiO_2 Fiber Photocatalysis in the Analysis of Dissolved Total Phosphate and the Degradation of Organophosphorous Pesticide," *Master's thesis, Nanjing Univ. Technol.*, 2006.

[63] W.K. Murphy, "The use of ozone in recycled oceanarium water," *New York Intl. Ozone Assoc. Pan Am. Group*, pp. 87–95, 1975.

[64] W.J. Blogoslowskii, "Water treatment by ozone in comparison with chlorinated water chlorination: environmental impact and health effects," *Ann Arbor Ann Arbor Sci.*, vol. 3, pp. 487–498, 1980.

[65] O.V. Kuz'mina, E.I. Potekhina, P. Yu., S.P. Peretyagin and Maslennikov, "Mechanism of the first step of ozone decomposition in aqueous solutions of sodium chloride in view of new data on the composition of reaction products," *Nizhegorod. Med. Zh.*, vol. 3, pp. 37–41, 1998.

[66] I.S. Boyarinov, G.A. Yakovlev, A. Yu., and Simutis, "Sposob povysheniya stabilnosti ozonirovannogo fiziologicheskogo rastvora," *Vestn. Fizioter. i Kurortol.*, vol. 5, pp. 14–16, 2004.

[67] L.R.B. Yeatts and H. Taube, "The Kinetics of the Reaction of Ozone and Chloride Ion in Acid Aqueous Solution," *J. Am. Chem. Soc.*, vol. 71, no. 12, pp. 4100–4105, 1949.

[68] V.V. Sizov, E.M. Piotrovskaya and E. Brodskaya, "Effect of the surface inhomogeneity of the adsorbent on the diffusion of methane in micropores," *Russ. J. Phys. Chem. A*, vol. 77, pp. 657–662, 2003.

[69] W.R. Haag and J. Hoign, "Ozonation of water containing chlorine or chloramines. Reaction products and kinetics," *Water Res.*, vol. 17, pp. 1397–1402, 1983.

[70] L.R.B. Yeatts and H. Taube, "The Kinetics of the Reaction of Ozone and Chloride Ion in Acid Aqueous Solution," *J. Am. Chem. Soc.*, vol. 71, no. 12, pp. 4100–4105, 1949.

[71] U.V. Gunten, "Ozonation of drinking water: Part I. Oxidation kinetics and product formation," *Water Res.*, vol. 37, no. 7, pp. 1443–1467, 2003.

[72] W.R. Haag, "On the disappearance of chlorine in sea-water," *Water Res.*, vol. 15, no. 7, pp. 937–940, 1981.

[73] I.V.K.E.A.V.L.A.V. Levanov, "The solubility of ozone and kinetics of its chemical reactions in aqueous solutions of sodium chloride," *Russ. J. Phys. Chem. A, Focus Chem.*, vol. 82, no. 12, pp. 2271–2276, 2008.

[74] S.D. Razumovskii, G.V. Korovina, and T.V. Grinevich, "Mechanism of the first step of ozone decomposition in aqueous solutions of sodium chloride in view of new data on the composition of reaction products," *Dokl. Phys. Chem.*, vol. 434, no. 2, pp. 163–165, 2010.

[75] S.D. Razumovskii, G.V. Korovina, and T.V. Grinevich, "Mechanism of the First Step of Ozone Decomposition in Aqueous Solutions of Sodium Chloride in View," *Phys. Chem.*, vol. 434, no. 4, pp. 493–495, 2010.

[76] Nikolskiy, *Nikolskiy, Spravochnik khimika (Chemist s Handbook)*. 1967.

[77] L.I. Komarova, N.N. Lapina, B.V. Lokshin, G.D. Markova and V.A. Vasnev, "Intermolecular interactions in the system of equilibrium catalytic transesterification of esters. Reaction of boron and arsenic butoxides with alcohols based on IR spectroscopic data," *Bull. Acad. Sci. USSR, Div. Chem. Sci.*, vol. 40, no. 2, pp. 321–324, 1991.

[78] S. D. R. S. O. L. K. E. Zaikov, "The kinetics of the reaction of ozone with hydroxyl ions in aqueous solution," *Bull. Acad. Sci. USSR, Div. Chem. Sci.*, vol. 25, no. 2, pp. 289–293, 1979.

[79] B. Mcelroy, "HO., NO, and ClO,: Their Role in Atmospheric Photochemistry," *Can. J. Chem.*, vol. 52, no. 8, pp. 1582–1591, 1973.

[80] J.T.R.J. Bull, L.S. Birnbaum, K.P. Cantor, J.B. Rose, B.E. Butterworth and R. Pegram, "Water chlorination : essential process or cancer hazard ?," *Fundam. Appl. Toxicol*, vol. 28, no. 2, pp. 155–166, 1995.

[81] R.C.S.G.A. Boorman, V. Dellarco, J.K. Dunnick, R.E. Chapin, S. Hunter, F. Hauchman, H. Gardner and M. Cox, "Drinking Water Disinfection Byproducs : Review and Approach to Toxicity Evaluation," *Environ. Heal. Perspect*, vol. 107, pp. 207–217, 1999.

[82] P.E.M.J. Nieuwenhuijsen, M.B. Toledano, N.E. Eaton and J. Fawell, "Chlorination disinfection byproducts in water and their association with adverse reproductive outcomes : a review," *Occup. Environ. Med.*, vol. 57, pp. 73–85, 2000.

[83] R.L. Wolfe, "Ultraviolet disinfection of potable water," *Environ. Sci. Technol.*, vol. 24, pp. 768–773, 1990.

[84] Alexandra, *WEF Wastewater disinfection. Manual of Practice FD-10.* 1996.

[85] C.A. Scott, "Ultraviolet disinfection of water," *Aqua*, vol. 2, pp. 109–115, 1984.

[86] G.R. Cairns, W.L. Sakamoto and G. Comair, "Assessing UVdisinfection of a physico-chemical effluent by medium pressure lamps using a collimated beam and pilot plant," *Proc. Water Environ. Fed. Spec. Conf. Planning, Des. Oper. Effl. Disinfect. Syst.*, pp. 433–444, 1993.

[87] F.M. Gehr and R. Cochrane, "Peracetic acid (PAA) as a disinfectant for municipal wastewaters: encouraging performance results from physicochemical as well as biological effluents," *Proc. Disinfect. 2002 Conf. Water Environ. Fed.*, pp. 17–20, 2002.

[88] M. Wj, "Ultraviolet light in water and wastewater sanitation," *Boca Rat. Lewis Publ.*, 2002.

[89] H. J. Oppenheimer, "Chlorine and UV disinfection of tertiary effluent: a comparative study of bacteria and viral inactivation and effluent by-products," *Proc. 66th Annu. Conf. Water Environ. Fed.*, pp. 557–568, 1993.

[90] R.R. Robson, "Wastewater ozonation in the USA—history and current status—1989," *Ozone Sci Eng*, vol. 13, pp. 23–40, 1991.

[91] P. Xu, M.L. Janex, P. Savoye, A. Cockx and V. Lazarova, "Wastewater disinfection by ozone: main parameters for process design," *Water Res.*, vol. 36, pp. 1043–1055, 2002.

[92] N.K. Hunt and B.J. Marinas, "Kinetics of Eschericia coli inactivation with ozone," *Water Res.*, vol. 31, no. 6, pp. 1355–1362, 1997.

[93] N. Wang, X. Zhang, Y. Wang, W. Yu, and H. L. W. Chan, "Microfluidic reactors for photocatalytic water purification.," *Lab Chip*, vol. 14, no. 6, pp. 1074–82, 2014.

[94] M. M. Khan *et al.* , "Band gap engineered TiO_2 nanoparticles for visible light induced photoelectrochemical and photocatalytic studies," *J. Mater. Chem. A*, vol. 2, no. 3, p. 637, 2014.

[95] J. Majewski, "Methods for measuring ozone concentration in ozone-treated water," *Prz. Elextrotechniczny*, no. 9, pp. 253–255, 2012.

[96] M.N. Chong, B. Jin, C W.K. Chow, and C. Saint, "Recent developments in photocatalytic water treatment technology: A review," *Water Res.*, vol. 44, no. 10, pp. 2997–3027, 2010.

[97] N. Wang, F. Tan, L. Wan, M. Wu, and X. Zhang, "Microfluidic reactors for visible-light photocatalytic water purification assisted with thermolysis," *Biomicrofluidics*, vol. 8, no. 5, pp. 1074–1082, 2014.

[98] D. Alibegic, S. Tsuneda, and A. Hirata, "Oxidation of Tetrachloroethylene in a Bubble Column Photochemical Reactor Applying the UV/H_2O_2 Technique," *Can. J. Chem. Eng.*, vol. 81, pp. 733–740, 2003.

[99] S. Gautam, S.P. Kamble, S.B. Sawant, and V.G. Pangarkar, "Photocatalytic degradation of 4-nitroaniline using solar and artificial UV radiation," *Chem. Eng. J.*, vol. 110, pp. 129–137, 2005.

[100] C. Guillard, H. Lachheb, A. Houas, M. Ksibi, E. Elaloui, and J.M. Herrmann, "Influence of chemical structure of dyes, of pH and of inorganic salts on their photocatalytic degradation by TiO_2 comparison of the efficiency of powder and supported TiO_2," *J. Photochem. Photobiol. A Chem.*, vol. 158, no. 1, pp. 27–36, 2003.

[101] P.K. Surolia, R.J. Tayade, and R.V Jasra, "Effect of Anions on the Photocatalytic Activity of Fe (III) Salts Impregnated TiO_2," *Society*, vol. 46, pp. 6196–6203, 2007.

[102] J. Kiwi, A. Lopez, and V. Nadtochenko, "Mechanism and kinetics of the OH^- radical intervention during Fenton oxidation in the presence of a significant amount of radical scavenger (Cl^-)," *Environ. Sci. Technol.*, vol. 34, no. 11, pp.

2162–2168, 2000.

[103] M. Abdullah, G. K.C. Low, and R.W. Matthews, "Effects of Common Inorganic Anions on Rates of Photocatalytic Oxidation of Organic Carbon over Illuminated Titanium Dioxide," *J . Phys. Chem*, vol. 94, no. 26, pp. 6820–6825, 1990.

[104] C. Kormann, D.W. Bahnemann, and M.R. Hoffmann, "Photolysis of Chloroform and Other Organic Molecules in Aqueous TiO, Suspensions," *Environ. Sci. Technol*, vol. 25, no. 3, pp. 494–500, 1991.

[105] D.F. Ollis, C.Y. Hsiao, L. Budiman, and C.L. Lee, "Heterogeneous photoassisted catalysis: Conversions of perchloroethylene, dichloroethane, chloroacetic acids, and chlorobenzenes," *J. Catal.*, vol. 88, no. 1, pp. 89–96, 1984.

[106] H.O. Ho and M. Co, *Criegee mechanism of ozonolysis*. Springer Berlin Heidelberg, 2006.

[107] R. Criegee, "Mechanism of Ozonolysis," *Angew. Chemie Int. Ed. English*, vol. 14, no. 11, pp. 745–752, 1975.

[108] L. Sánchez, J. Peral, and X. Domènech, "Aniline degradation by combined photocatalysis and ozonation," *Appl. Catal. B Environ.*, vol. 19, no. 1, pp. 59–65, 1998.

[109] R. Society, "Experiments on the Quantity of Gases Absorbed by Water, at Different Temperatures, and under Different Pressures," *Philos. Trans. R. Soc. London*, vol. 93, pp. 29-42-276, 1802.

[110] R. Battino, T.R. Rettich, and T. Tominaga, "The Solubility of Nitrogen and Air in Liquids," *J. Phys. Chem. Ref. Data*, vol. 13, no. 2, pp. 563–600, 1984.

[111] S. Morooka, K. Ikemizu, H. Kamano and Y. Kato, "Ozonation Rate of Water-

Soluble Chelates and Related Compounds," *J. Chem. Eng. Japan*, vol. 19, pp. 294–299, 1986.

[112] J. J. Wu and S. J. Masten, "Mass Transfer of Ozone in Semibatch Stirred Reactor," *J. Environ. Eng.*, pp. 1089–1099, 2001.

[113] L.F.K. Channing and G.R. Helz, "Solubility of Ozone in Aqueous Solutions of 0 -0.6M Ionic Strength at 5-30℃," *Environ. Scl. Technol.*, vol. 17, no. 3, pp. 145–149, 1983.

[114] V. Caprio, A. Insola, P. G. Lignola, and G. Volpicelli, "A new attempt for the evaluation of the absorption constant of ozone in water," *Chem. Engng Sci.*, vol. 37, pp. 122–123, 1982.

[115] Andrzej Konrad Bińi, "Ozone Solubility in Liquids," *Ozone Science and Engineering*, 28(2), pp. 67-75, 2006.

[116] J. L. Sotelo, F. J. Beltrán, M. González, and J. Domínguez, "Effect of high salt concentrations on ozone decomposition in water," *J. Environ. Sci. Heal. . Part A Environ. Sci. Eng.*, vol. 24, no. 7, pp. 823–842, 1989.